arXiv:1704.02617v1 [nucl-th] 9 Apr 2017

A New Paradigm for Hadronic Parity Nonconservation and its Experimental Implications

Susan Gardner[a,d], W. C. Haxton[b,d], and Barry R. Holstein[c,d]

[a]Department of Physics and Astronomy,
University of Kentucky, Lexington, KY 40506

[b]Department of Physics, University of California, and
Lawrence Berkeley National Laboratory, Berkeley, CA 94720

[c]Department of Physics-LGRT
University of Massachusetts, Amherst, MA 01003

[d]Kavli Institute for Theoretical Physics
University of California, Santa Barbara, CA 93016

April 11, 2017

Abstract

For decades the primary experimental goal in studies of hadronic parity nonconservation (PNC) has been the isolation of the isovector weak nucleon-nucleon interaction, expected to be dominated by long-range pion exchange and enhanced by the neutral current. In meson-exchange descriptions this interaction together with an isoscalar interaction generated by ρ and ω exchange dominate most observables. Consequently these two amplitudes have been used to compare and check the consistency of the field's experiments. Yet to date, despite sensitive searches like that performed with ^{18}F, no evidence for isovector hadronic PNC has been found. Here we argue, based on recent large-N_c treatments and new global analyses, that the emphasis on isovector hadronic PNC was misplaced. Large-N_c provides an alternative and theoretically better motivated simplification of effective field theories (EFTs) of hadronic PNC, separating the five low-energy constants (LECs) into two of leading order (LO), and three others that are N^{2}LO. This scheme pivots the isospin coordinates we have traditionally used, placing one dominant axis in the isoscalar plane, and a second along the isotensor direction. We show that this large-N_c LEC hierarchy accurately describes all existing data on hadronic PNC. In particular, the null result found in ^{18}F reflects its dependence on an N^{2}LO observable. We discuss opportunities to further test the predicted large-N_c hierarchy of LECs, illustrating the kind of analyses experimentalists can use to better constrain the LO theory and to determine the size of N^{2}LO corrections. This formalism – combined with a new wave of experiments that will be performed at the SNS cold neutron beam line and the recent demonstration that lattice QCD can now be applied to PNC NN scattering – could lead to rapid progress in the next five years. We discuss the impact of anticipated new results, including NPDGamma and a lattice QCD calculation of isotensor PNC. We also describe future experiments that can yield more precise values of the LO LECs and help isolate the N^{2}LO $\sim 10\%$ corrections.

1 Introduction

For more than two decades the field of hadronic parity nonconservation (PNC) has struggled: the theoretical picture has been muddled, and very few new experiments have been done to help clarify matters. This situation is about to change. The creation of a high-intensity cold neutron beamline at the Spallation Neutron Source (SNS) as well as upgrades at NIST will enable a new generation of experiments. Results from the first experiment performed at the SNS, the NPDGamma Collaboration's measurement of the gamma ray asymmetry $A_\gamma(\vec{n}p \to d\gamma)$, should be announced soon [1, 2, 3]. Furthermore, the feasibility of a new kind of "measurement" – evaluation of PNC NN scattering amplitudes from lattice QCD – has been demonstrated [4].

While such progress was being made, other developments have brought more clarity to the field, changing some of our prejudices, and providing a new context for interpreting future results. First, it was discovered that the agreement between past experiments was better than had been recognized [5]: most of the tension that had existed was induced by flaws in global analyses of PNC. Second, a new proposal emerged for organizing the low-energy constants (LECs) that characterize hadronic PNC, based on large-N_c QCD [6, 7]. We show here that this proposal accounts simply for all existing data – while illustrating that some of our past prejudices about hadronic PNC patterns were not justified. We describe these developments, and discuss their implications for past and anticipated experiments, performing a new global experimental analysis that exploits the large-N_c LEC hierarchy.

NPDGamma is the latest effort to address one of the field's primary goals, measurement of PNC in the isovector nucleon-nucleon (NN) interaction. In meson-exchange descriptions this interaction is dominated by long-range pion-exchange, with one πNN vertex governed by the weak interaction and the other by the strong. The weak πNN vertex h_π^1 has been of particular interest because of the expectation it could help separate the roles of W- and Z-exchange in hadronic PNC, associated with the four-currents J_W and J_Z that appear in the low-energy current-current Hamiltonian [8, 9]

$$\mathcal{H} = \frac{G_F}{\sqrt{2}} \left[J_W^\dagger J_W + J_Z^\dagger J_Z \right]. \tag{1}$$

The charged current can be decomposed into two components, $J_W = \cos\theta_c J_W^0 + \sin\theta_c J_W^1$, where θ_c is the Cabibbo angle. The current J_W^0 drives the $u \to d$ transition and carries isospin and strangeness $\Delta I = 1$, $\Delta S = 0$, while J_W^1 drives the $u \to s$ transition and carries $\Delta I = \frac{1}{2}$, $\Delta S = -1$. The neutral current also has two components, $J_Z = J_Z^0 + J_Z^1$, transforming as $\Delta I = 0$, $\Delta S = 0$ and $\Delta I = 1$, $\Delta S = 0$, respectively. The current-current weak $\Delta S = 0$ NN interaction is then

$$\mathcal{H}^{\Delta S=0} = \frac{G_F}{\sqrt{2}} \left[\cos^2\theta_c J_W^{0\dagger} J_W^0 + \sin^2\theta_c J_W^{1\dagger} J_W^1 + J_Z^{0\dagger} J_Z^0 + J_Z^{1\dagger} J_Z^1 + J_Z^{0\dagger} J_Z^1 + J_Z^{1\dagger} J_Z^0 \right]. \tag{2}$$

The importance of isospin to this Lagrangian is clear: the symmetric product of two $\Delta I = 1$ J_W^0 currents transforms as $\Delta I = 0$ and 2, while the symmetric product of two $\Delta I = \frac{1}{2}$ J_W^1 currents transforms as $\Delta I = 1$. Consequently the charged-current contribution to the $\Delta I = 1$ weak NN interaction is suppressed by $\tan^2\theta_c \sim 0.04$, relative to the charged-current contributions to the $\Delta I = 0$ and 2 interactions. Based on this argument it was concluded that the $\Delta I = 1$ component of the NN interaction would be dominated by the neutral current, which is of particular interest because it cannot be studied in strangeness-changing interactions due to the absence of tree-level flavor-changing neutral currents. The expectation of an important neutral current contribution to the $\Delta I = 1$ PNC NN interaction has influenced PNC analyses since the 1980s.

The opportunity to take advantage of nuclei as laboratories to test an otherwise unconstrained standard-model interaction has motivated both experiment and theory. By the mid-1980s several advances had occurred:

1. Credible meson-exchange models of HPNC had been developed that established "best values" and reasonable ranges for hadronic PNC weak couplings (e.g., the DDH couplings of Desplanques, Donoghue, and Holstein [10]), including h_π^1;

2. A series of successful experiments measuring the circular polarization of the gamma ray from the decay of the 1.081 MeV $J^PT=0^-0$ level in ^{18}F had been performed, testing the T=1 mixing of this state with the nearby 0^+1 level at 1.042 MeV [11, 12, 13, 14, 15], but finding no signal at the $\sim 10^{-4}$ level; and

3. A method to extract a limit on h_π^1 from these measurements was developed, exploiting a relationship between hadronic PNC and axial-charge β-decay, largely eliminating any dependence on the choice of nuclear wave functions [16, 17, 18]. Several high-quality measurements of the β decay rate were made [18].

This led to a surprising conclusion: the ^{18}F result, by itself or when combined with other measurements in a general hadronic PNC analysis [19], established an upper bound on h_π^1, relative to competing isoscalar amplitudes, about a factor of six below the DDH best value. The isoscalar amplitudes are somewhat stronger than expected, and the isovector considerably weaker. The analogy between this result and the $\Delta I = \frac{1}{2}$ rule in strangeness-changing decays – where a similar anomaly in the ratio of $\Delta I = \frac{3}{2}$ to $\Delta I = \frac{1}{2}$ amplitudes is found – was immediately noted [19]. These results show that the neutral current, once embedded in the strongly interacting environment of the nucleon, produces an effective coupling to the nucleon considerably weaker than that expected from the elementary coupling to the quarks.

These results helped motivate the NPDGamma effort. The Collaboration has worked toward its goal of measuring h_π^1 since approximately 2000, beginning with an earlier version of the experiment at LANSCE [20], then moving to the SNS to exploit the high-intensity cold neutron beamline that became available there [1, 2, 3]. The goal has been to reach a sensitivity corresponding to $A_\gamma \sim 10^{-8}$ [21], verifying the ^{18}F result and possibly pushing beyond, to a detection of h_π^1. Experimental issues at LANSCE, including a weaker than anticipated neutron flux, led to a final result of $A_\gamma = (-1.2 \pm 2.1(\mathrm{stat}) \pm 0.2(\mathrm{sys})) \times 10^{-7}$ [20]. The effort to reach the 10^{-8} level was renewed on the high-intensity SNS beamline [22]. The DDH best-value prediction for A_γ is $\sim 5 \times 10^{-8}$.

The purpose of this paper is to re-examine past experiments and consider anticipated new results, including those from NPDGamma, in the context of a new paradigm for hadronic PNC that arises when effective field theory (EFT) is combined with large-N_c instructions for treating the EFT's LECs. In the context of this scheme, not only ^{18}F but the entire set of hadronic PNC observations conform to a simple pattern. The purpose of this article is describe recent developments that have led to this satisfying conclusion. These include

1. Modified constraints [5] extracted from the longitudinal asymmetry $A_L(\vec{\mathrm{p}}\mathrm{p})$, at both low and intermediate energies, obtained when certain inconsistencies in past global hadronic PNC analyses were corrected.

2. An improved understanding of EFT approaches to hadronic PNC, ironing out some apparent differences between EFT descriptions [23, 24, 25] as well as establishing their effective equivalence to the traditional meson exchange treatment, when the latter is restricted to low energies. The EFT approach leads to a description quite similar to Danilov's [26, 27, 28] early analysis in terms of S-P amplitudes, involving five degrees of

freedom (or perhaps six if nuclear systems like ^{18}F are used, where the pion's range is important).

3. As we lack the data needed to perform a five- or six-dimensional analysis, the field has long employed simpler analyses with a smaller number of "most important" couplings. In the DDH meson-exchange model, h^1_π and a corresponding vector-meson isoscalar coupling have been employed as the leading terms. However, as we will discuss, this choice is both in conflict with experiment and lacking in theoretical justification. Recently an alternative organizational scheme has been proposed, based on the large N_c expansion, that appears to be compatible with all we have learned about hadronic PNC to date. This expansion identifies two alternative leading couplings, and predicts that subleading corrections to this scheme will enter at the relative order $1/N_c^2 \sim 10\%$.

4. This combined EFT/large-N_c approach leads to a lowest-order (LO) two-dimensional (2D) characterization of hadronic PNC that uses the isotensor $^1S_0 - {}^3P_0$ amplitude together with a specific combination of the isoscalar $^3S_1 - {}^1P_1$ and $^1S_0 - {}^3P_0$ amplitudes. We derive the LO LECs from current experiments, and show the general concordance between PNC observations and the coupling hierarchy predicted by the large-N_c scheme.

5. We describe further opportunities to further test this picture, through new experiments and by using lattice QCD.

6. The ^{18}F and NPDGamma experiments probe observables that are blind to the LO couplings, and thus arise only through N^{2}LO corrections. Thus the absence of a ^{18}F signal is not in conflict with theory, but is in fact consistent with large-N_c predictions. We show that by combining the ^{18}F result with the anticipated NPDGamma measurement, important constraints can be placed on N^{2}LO couplings.

This paper reviews the first three developments above, then addresses the last three points by performing a new global analysis using the EFT/large-N_c formalism.

2 Background

The violation of parity invariance, suggested by Lee and Yang in 1956 [29], was discovered experimentally in 1957 by Wu et al. via measurement of the $\boldsymbol{J} \cdot \boldsymbol{p}_e$ correlation parameter in the beta decay of oriented ^{60}Co [30]. It was immediately recognized that there should exist a corresponding PNC component of the NN interaction. The first experimental search for PNC was conducted by Tanner, who in 1957 sought evidence in the $^{19}\mathrm{F}(p,\alpha)^{16}\mathrm{O}$ reaction [31]. Although the sensitivity of this measurement was not sufficient to observe a PNC signal, it was the first of a series of such experiments that have continued to the present time, to detect subtle weak interaction effects in systems with strong and electromagnetic interactions. A summary can be found in various review articles [19, 32, 33, 5]. PNC has been observed in many hadronic systems, usually in the form of some pseudoscalar such as an asymmetry or a circular polarization, including cases where rather spectacular enhancements of the signal arise. Examples include the 2% photon circular polarization in the electromagnetic decay of an isomer of ^{180}Hf [34]

$$A_\gamma(^{180}\mathrm{Hf}^* \to {}^{180}\mathrm{Hf} + \vec{\gamma}) = -(1.66 \pm 0.18) \times 10^{-2}, \tag{3}$$

and the nearly 10% longitudinal analyzing power for the scattering of polarized neutrons from ^{139}La [35]

$$A_h(\vec{n} + {}^{139}\mathrm{La}) = (9.55 \pm 0.35) \times 10^{-2}. \tag{4}$$

These amplifications originate from chance nuclear level near degeneracies: states of the same spin but opposite parity can mix through the hadronic PNC interaction, generating a parity admixture inversely proportional to the energy splitting between the levels. Indeed, as the natural scale of hadronic PV effects is $\sim G_F m_\pi^2 \sim 10^{-7}$ [19], it is apparent that such enhancements can be many orders of magnitude.

With the development of theoretical frameworks for understanding hadronic PNC quantitatively, the field's attention switched from simply finding examples of PNC, to identifying systems where PNC could be both measured and reliably interpreted in terms of the underlying PNC NN interaction. In an ideal world such measurements would be carried out by studying the simple NN systems – pp, np, and pn – in the allowed threshold partial-wave channels. As only one such measurement has been done at high precision, the field turned to few-nucleon systems, where techniques exist for solving the Schrödinger equation with realistic strong potentials. Certain selected light nuclei also provided reliable hadronic PNC constraints. Notable among these are ^{18}F and ^{19}F, where parity doublets enhance the experimental signal, and axial-charge beta decay measurements can remove almost all of the usual nuclear structure uncertainties.

2.1 The DDH potential

Helping to drive these developments were theoretical descriptions of hadronic PNC defining what needed to be measured, and providing benchmark estimates of potential hadronic PNC signal sizes. The "standard" formalism for hadronic PNC experimental analysis became the meson exchange model of Desplanques, Donoghue, and Holstein (DDH) [10], which expresses the hadronic PNC potential in terms of the usual parity-conserving strong interaction meson-nucleon couplings defined by

$$\begin{aligned}\mathcal{H}_{\rm st} &= i g_{\pi NN}\bar{N}\gamma_5 \boldsymbol{\tau}\cdot\boldsymbol{\pi} N + g_\rho \bar{N}\left(\gamma_\mu + i\frac{\chi_\rho}{2m_N}\sigma_{\mu\nu}k^\nu\right)\boldsymbol{\tau}\cdot\boldsymbol{\rho}^\mu N \\ &\quad + g_\omega \bar{N}\left(\gamma_\mu + i\frac{\chi_\omega}{2m_N}\sigma_{\mu\nu}k^\nu\right)\omega^\mu N, \end{aligned} \tag{5}$$

where m_N is the nucleon mass. The numerical values assigned to the various couplings by DDH are $g_{\pi NN}^2/4\pi = 14.4$, $g_\rho^2/4\pi = \frac{1}{9}g_\omega^2/4\pi = 0.62$, $\chi_\rho = \kappa_p - \kappa_n = 3.70$, and $\chi_\omega = \kappa_p + \kappa_n = -0.12$. DDH employed the phenomenological PNC weak meson-nucleon Hamiltonian

$$\begin{aligned}\mathcal{H}_{\rm wk} &= i\frac{h_\pi^1}{\sqrt{2}}\bar{N}(\boldsymbol{\tau}\times\boldsymbol{\pi})_z N \\ &+ \bar{N}\left(h_\rho^0\boldsymbol{\tau}\cdot\boldsymbol{\rho}^\mu + h_\rho^1\rho_z^\mu + \frac{h_\rho^2}{2\sqrt{6}}(3\tau_z\rho_z^\mu - \boldsymbol{\tau}\cdot\boldsymbol{\rho}^\mu)\right)\gamma_\mu\gamma_5 N \\ &+ \bar{N}\left(h_\omega^0\omega^\mu + h_\omega^1\tau_z\omega^\mu\right)\gamma_\mu\gamma_5 N - h_\rho^{\prime 1}\bar{N}(\boldsymbol{\tau}\times\boldsymbol{\rho}^\mu)_z\frac{\sigma_{\mu\nu}k^\nu}{2m_N}\gamma_5 N. \end{aligned} \tag{6}$$

When Eqs. (5) and (6) are combined and a nonrelativistic reduction is made, a PNC potential is obtained with a specific spin and isospin structure, together with specific radial forms, governed by the meson masses. The coefficients of this potential are bilinears in the weak and strong couplings – these products are the parameters that can be extracted.

Provided a consistent set of strong couplings is employed in global analyses, such a program would determine values for the weak couplings $h_\pi^1, h_\rho^{0,1,2}, h_\rho^{1\prime}, h_\omega^{1,2}$. In their original work DDH provided theoretical estimates for these parameters – while emphasizing their *very* large uncertainties. DDH provided a best guess for each parameter (called by these authors the "best value"), as well as a "reasonable range" to provide a measure of the uncertainty, as shown in Table 1.

Table 1: The weak meson-nucleon couplings as estimated in Refs. [10, 36, 37]. All numbers are quoted in units of 10^{-7}. Following the original treatment by DDH, h'^1_ρ has been set to zero: it can be shown at low energies that this coupling is redundant [5].

Coupling	DDH [10] Reasonable Range	DDH [10] "Best" Value	DZ [36]	FCDH [37]
h^1_π	$0 \to 11$	$+4.6$	$+1.1$	$+2.7$
h^0_ρ	$11 \to -31$	-11	-8.4	-3.8
h^1_ρ	$-0.4 \to 0$	-0.2	$+0.4$	-0.4
h^2_ρ	$-7.6 \to -11$	-9.5	-6.8	-6.8
h^0_ω	$5.7 \to -10.3$	-1.9	-3.8	-5.0
h^1_ω	$-1.9 \to -0.8$	-1.2	-2.3	-2.3

Despite a great deal of experimental and theoretical work, most of this uncertainty remains today. The main obstacle to reducing the reasonable ranges has been a lack of reliable experimental constraints. Critical examinations of the available data have led to the conclusion that only four experiments place important constraints on hadronic PNC – the analyzing power for the scattering of longitudinally polarized protons off protons, the circular polarization of the gamma ray emitted from the 0^-0 excited state in ^{18}F, the analyzing power for the scattering of longitudinally polarized protons off ^{4}He, and the gamma decay asymmetry from the decay of the polarized $\frac{1}{2}^-\frac{1}{2}$ state in ^{19}F. The last two measurements both involve odd-proton systems, and consequently yield almost the same constraint, while the ^{18}F result is only an upper bound (though a very significant one, given the DDH best-value estimate of the best value for h^1_π).

To improve on the current situation, one needs either several new, interpretable experimental results, or a strategy that reduces the number of theoretical variables that must be determined. Such a strategy has recently been proposed, based in large-N_c QCD. As this approach is most naturally described in terms of effective field theory treatments of hadronic PNC, we first describe that formalism and its relationship to the DDH potential.

2.2 The EFT Picture

While the DDH meson-exchange approach clearly contains some model dependence, it has stood as the standard language for analyzing low energy PNC experiments for nearly four decades. In recent years, however, an alternative to the DDH potential has been developed, based on pionless effective field theory. Pionless EFT provides a model-independent formalism for describing experiments performed at momentum scales well below the pion mass, where the pion interaction becomes local. Most applications to PNC scattering satisfy this condition [38], at least with respect to the external momenta of the scattered particles. (If a nuclear bound state is involved, however, the nuclear Fermi momentum can also play a role.)

This approach was introduced in studies of hadronic PNC by Zhu et al. [23], though the roots of this kind of analysis reach back to Danilov's partial wave analysis [26, 27] and to the use of contact potentials by Desplanques and Missimer [39]. The Zhu et al. formulation contained redundant terms that were later identified and eliminated by Girlanda [24]. The EFT method was also developed in the work of Phillips, Schindler, and Springer [25]. In pionless EFT the NN interaction is represented by a small number of empirically determined contact terms. In the parity-conserving case, for example, there are only two, representing scattering lengths in the $^1S_0$ and $^3S_1$ channels. In the parity-violating case, however, there exist *five* low-energy S-P channels, and consequently five associated LECs.

While the DDH and EFT approaches appear to be quite distinct, in fact they are op-

erationally equivalent at the very low energies where pionless EFT is valid. This point was recently made by constructing an effective contact interaction that maps onto Danilov's partial wave analysis [5]

$$
\begin{aligned}
V_{LO}^{PNC}(\boldsymbol{r}) &= \Lambda_0^{^1S_0-{}^3P_0}\left(\frac{1}{i}\frac{\overleftrightarrow{\boldsymbol{\nabla}}_A}{2m_N}\frac{\delta^3(\boldsymbol{r})}{m_\rho^2}\cdot(\boldsymbol{\sigma}_1-\boldsymbol{\sigma}_2)-\frac{1}{i}\frac{\overleftrightarrow{\boldsymbol{\nabla}}_S}{2m_N}\frac{\delta^3(\boldsymbol{r})}{m_\rho^2}\cdot i(\boldsymbol{\sigma}_1\times\boldsymbol{\sigma}_2)\right)\\
&+ \Lambda_0^{^3S_1-{}^1P_1}\left(\frac{1}{i}\frac{\overleftrightarrow{\boldsymbol{\nabla}}_A}{2m_N}\frac{\delta^3(\boldsymbol{r})}{m_\rho^2}\cdot(\boldsymbol{\sigma}_1-\boldsymbol{\sigma}_2)+\frac{1}{i}\frac{\overleftrightarrow{\boldsymbol{\nabla}}_S}{2m_N}\frac{\delta^3(\boldsymbol{r})}{m_\rho^2}\cdot i(\boldsymbol{\sigma}_1\times\boldsymbol{\sigma}_2)\right)\\
&+ \Lambda_1^{^1S_0-{}^3P_0}\left(\frac{1}{i}\frac{\overleftrightarrow{\boldsymbol{\nabla}}_A}{2m_N}\frac{\delta^3(\boldsymbol{r})}{m_\rho^2}\cdot(\boldsymbol{\sigma}_1-\boldsymbol{\sigma}_2)(\tau_{1\,z}+\tau_{2\,z})\right)\\
&+ \Lambda_1^{^3S_1-{}^3P_1}\left(\frac{1}{i}\frac{\overleftrightarrow{\boldsymbol{\nabla}}_A}{2m_N}\frac{\delta^3(\boldsymbol{r})}{m_\rho^2}\cdot(\boldsymbol{\sigma}_1+\boldsymbol{\sigma}_2)(\tau_{1\,z}-\tau_{2\,z})\right)\\
&+ \Lambda_2^{^1S_0-{}^3P_0}\left(\frac{1}{i}\frac{\overleftrightarrow{\boldsymbol{\nabla}}_A}{2m_N}\frac{\delta^3(\boldsymbol{r})}{m_\rho^2}\cdot(\boldsymbol{\sigma}_1-\boldsymbol{\sigma}_2)(\boldsymbol{\tau}_1\otimes\boldsymbol{\tau}_2)_{20}\right), \qquad (7)
\end{aligned}
$$

where $(\boldsymbol{\tau}_1\otimes\boldsymbol{\tau})_{20}\equiv(3\tau_{1\,z}\tau_{2\,z}-\boldsymbol{\tau}_1\cdot\boldsymbol{\tau}_2)/\sqrt{6}$. The subscripts on the LECs denote the change in isospin ΔI induced by the associated operator, while the superscripts indicate the specific PNC transition. With these operator definitions the various Λs are dimensionless. Of course, there must exist a matching to the low-energy form of the DDH potential, yielding [5]

$$
\begin{aligned}
\Lambda_0^{^1S_0-{}^3P_0} &= -g_\rho(2+\chi_\rho)h_\rho^0-g_\omega(2+\chi_\omega)h_\omega^0 && {}^{\rm DDH}\Lambda_0^{^1S_0-{}^3P_0}=210\\
\Lambda_0^{^3S_1-{}^1P_1} &= -3g_\rho\chi_\rho h_\rho^0+g_\omega\chi_\omega h_\omega^0 && {}^{\rm DDH}\Lambda_0^{^3S_1-{}^1P_1}=360\\
\Lambda_1^{^1S_0-{}^3P_0} &= -g_\rho(2+\chi_\rho)h_\rho^1-g_\omega(2+\chi_\omega)h_\omega^1 && {}^{\rm DDH}\Lambda_1^{^1S_0-{}^3P_0}=21\\
\Lambda_1^{^3S_1-{}^3P_1} &= \sqrt{\tfrac{1}{2}}\,g_{\pi NN}\left(\tfrac{m_\rho}{m_\pi}\right)^2 h_\pi^1+g_\rho(h_\rho^1-h_\rho^{1\prime})-g_\omega h_\omega^1 && {}^{\rm DDH}\Lambda_1^{^3S_1-{}^3P_1}=1340\\
\Lambda_2^{^1S_0-{}^3P_0} &= -g_\rho(2+\chi_\rho)h_\rho^2 && {}^{\rm DDH}\Lambda_2^{^1S_0-{}^3P_0}=160 \qquad (8)
\end{aligned}
$$

where on the right the DDH predicted "best values" have been employed, yielding values for the LECs (units of 10^{-7}). Similarly, the EFT potentials of Girlanda et al. [24] and Zhu et al. [23] must also be equivalent to Eq. (7). The translation between the various formulations is given in the "Rosetta stone" Table 2 in [5].

This comparison shows that the DDH potential is effectively equivalent to pionless EFT at the low energies for which the latter is valid. In this regime an S-P partial wave description is adequate, and five linear combinations of the seven DDH weak couplings describe the physics. The redundancy among these parameters is broken when P-D interactions become important. Then the meson masses also play an explicit role, as higher partial wave channels allow one to detect the non-contact form of the radial interaction. One can think of the DDH interaction as an EFT that is married to a physically motivated model, for the purpose extending the interaction's range of validity to higher momenta.

However, regardless of what formulation one uses, there remains a major problem: five parameters are needed to describe hadronic PNC in the low-momentum limit, but we do not have five reliable experimental constraints. Thus some simplification is needed, beyond that provided by EFT or by a low-momentum reduction of the DDH potential.

2.3 Experimental Constraints and 2D Reductions

A standard display of experimental constraints on hadronic PNC was introduced in [19] and has been in broad use ever since. It employs two parameters, not five, and was derived on

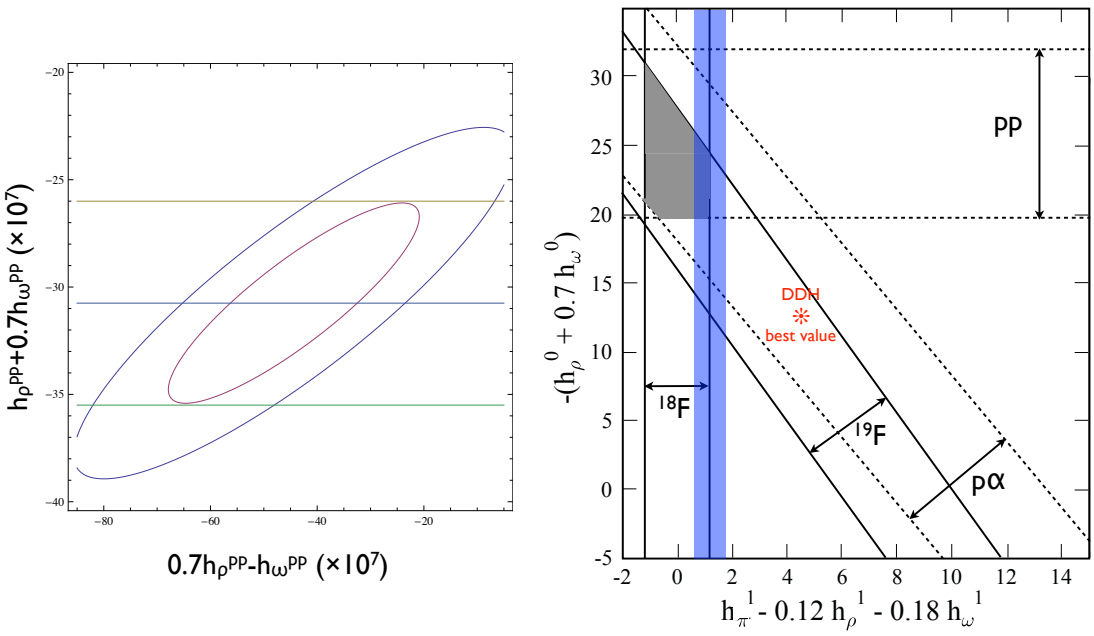

Figure 1: Right panel: the standard plot of experimental constraints on the DDH parameters, including recent revisions introduced in [5]. The experimental bands are 1σ. The blue band comes from a preliminary estimate of h_π^1, based on a lattice QCD calculation of a three-point function [40], as discussed in the text. Left panel: constraints on $h^{pp}_{\rho,\omega} = h^0_{\rho,\omega} + h^1_{\rho,\omega} + h^2_{\rho,\omega}/\sqrt{6}$ derived from $A_L(\vec{p}p)$ [5, 41]. The ellipses are the 68% and 90% c.l. contours.

largely empirical grounds – an after-the-fact examination of how theoretical predictions of PNC observables depend on the underlying weak couplings. In light of subsequent discussions we will have of the large-N_c expansion, we sketch here how this standard display came about.

The current version of this plot is shown in Fig. 1. It includes constraints from four experiments:

1. The longitudinal analyzing power in the scattering of polarized protons from an unpolarized proton target, for which measurements were performed at 13.6 MeV at Bonn, 15 MeV at LANL, 45 MeV at PSI, and 221 MeV at TRIUMF,

$$A_L(\vec{p}p) = \begin{cases} (-0.93 \pm 0.20 \pm 0.05) \times 10^{-7} & 13.6\,\text{MeV}\ [42] \\ (-1.7 \pm 0.8) \times 10^{-7} & 15\,\text{MeV}\ [43] \\ (-1.57 \pm 0.23) \times 10^{-7} & 45\,\text{MeV}\ [44,\ 45,\ 46] \\ (0.84 \pm 0.34) \times 10^{-7} & 221\,\text{MeV}\ [47,\ 48] \end{cases} . \tag{9}$$

The first three experiments were done at relatively low energy, where a description in terms of S-P amplitudes is a reasonable approximation. Thus they constrain the partial wave coefficients of Eq. (7) in a straightforward way [5, 41],

$$\Lambda_0^{^1S_0-{}^3P_0} + \Lambda_1^{^1S_0-{}^3P_0} + \frac{1}{\sqrt{6}}\Lambda_2^{^1S_0-{}^3P_0} = 419 \pm 43\ . \tag{10}$$

The S-P LECs Λ are given in units of 10^{-7}. The TRIUMF measurement, in contrast, must be treated in a formalism that includes higher partial waves in the weak interaction, such as the DDH potential. As indicated in the left panel of Fig. 1, the resulting constraints on

weak couplings can be expressed in terms of one combination related to S-P amplitudes, using the relations in Eq. (8), and another associated with P-D amplitudes. We will discuss this result in more detail below.

2. The longitudinal analyzing power for scattering 46 MeV polarized protons on a ^{4}He target was measured at PSI [49, 50]

$$A_L(\vec{\mathrm{p}}\alpha)\big|_{46\mathrm{MeV}} = -(3.3 \pm 0.9) \times 10^{-7}, \tag{11}$$

placing the following constraint on the S-P LECs [49, 5]

$$\Lambda_0^{^1S_0-^3P_0} + 0.89\Lambda_1^{^1S_0-^3P_0} + 0.75\Lambda_0^{^3S_1-^1P_1} + 0.32\Lambda_1^{^3S_1-^3P_1} = 930 \pm 253\ . \tag{12}$$

3. The circular polarization of photons emitted in the decay of the 1.081 MeV 0^-0 excited state of ^{18}F to the 1^+0 ground state is induced by PNC mixing of the 0^- state with the nearby 0^+1 state at 1.042 MeV (see Fig 2). Consequently this experiment selects out isovector hadronic PNC. Four independent experiments have yielded the limits

$$P_\gamma = \begin{cases} (-7 \pm 20) \times 10^{-4} & \text{Caltech/Seattle [11]} \\ (-10 \pm 18) \times 10^{-4} & \text{Mainz [13]} \\ (3 \pm 6) \times 10^{-4} & \text{Florence [14]} \\ (2 \pm 6) \times 10^{-4} & \text{Queens [15]} \end{cases} . \tag{13}$$

These results lead to the constraint [16, 5]

$$|\Lambda_1^{^3S_1-^3P_1} + 2.42\Lambda_1^{^1S_0-^3P_0}| < 340, \tag{14}$$

which implies a value of h_π^1 significantly below the DDH best value.

4. The gamma decay angular asymmetry for the transition from the polarized 110 keV $\frac{1}{2}^-$ excited state in ^{19}F to the $\frac{1}{2}^+$ ground state has been measured, testing the parity mixing of these levels (see Fig. 2). The results

$$A_\gamma = \begin{cases} (-8.5 \pm 2.6) \times 10^{-5} & \text{Seattle [18]} \\ (-6.8 \pm 1.8) \times 10^{-5} & \text{Mainz [51, 52]} \end{cases} \tag{15}$$

constrain isoscalar and isovector hadronic PNC [18, 5]

$$\Lambda_0^{^1S_0-^3P_0} + 0.67\Lambda_1^{^1S_0-^3P_0} + 0.43\Lambda_0^{^3S_1-^1P_1} + 0.29\Lambda_1^{^3S_1-^3P_1} = 661 \pm 169\ . \tag{16}$$

Note that this constraint is quite similar to that obtained from $\vec{\mathrm{p}}$+^{4}He: both systems involve an unpaired proton. As with ^{18}F, the nuclear mixing matrix element used in the analysis was determined from the axial-charge β decay of ^{19}Ne, linking the same states (up to an isospin rotation). The details of this determination can be found in [18].

The plot omits other constraints either because their interpretation is uncertain, or because the measurement that have been done lack the precision needed to place meaningful constraints on hadronic PNC. Examples of the former include the anapole moment measurement for ^{133}Cs [53] and the circular polarization of the 2.789 MeV γ ray emitted in the decay of ^{21}Ne [54, 55]. The interpretations of these experiments depend on shell model estimates of quite complicated polarizabilities (Cs) or suppressed mixing matrix elements (^{21}Ne), and there are reasons to believe the associated errors could be large [5]. The plot also omits hadronic PNC constraints established in experiments on neutron spin rotation in ^{4}He [56], on the longitudinal analyzing

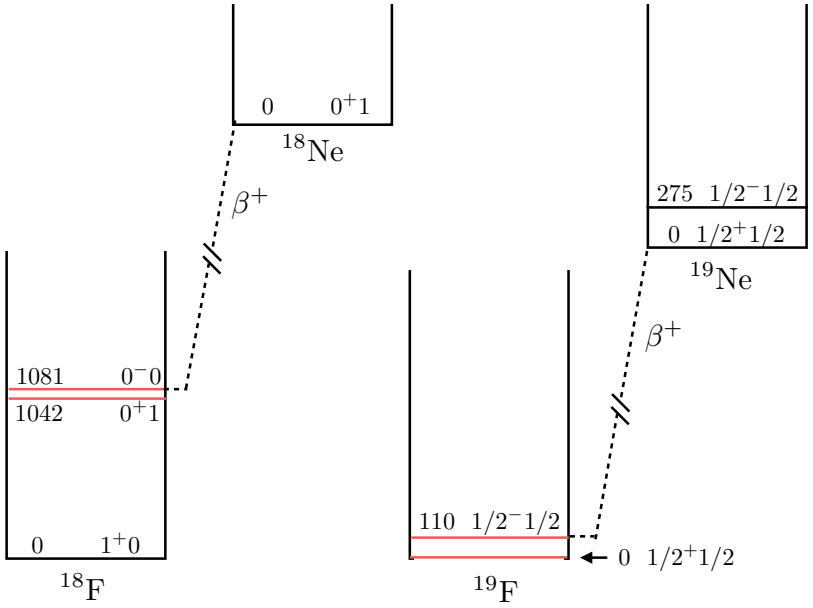

Figure 2: The parity doublets in ^{18}F and ^{19}F are indicated in red. The β^+ decays from ^{18}Ne and ^{19}Ne connect the negative-parity members of the parity doublets to the isotopic analogs of the positive-parity members (the ground states of ^{18}Ne and ^{19}Ne). These axial-charge β^+ decays can be used to calibrate the strength of the PNC doublet mixing. Energies are in keV.

power for the capture of polarized protons on deuterium [43], on the circular polarization of γ-rays produced in the capture of unpolarized neutrons on deuterium nd $\rightarrow$ tγ [57], and on the γ-ray asymmetry from the capture of polarized neutrons on deuterium [58] . The first three experiments established upper bounds that are not sufficiently restrictive to impact our analysis. The fourth experiment produced a signal much larger than expected, and for that reason is widely thought to reflect an unidentified experimental systematic.

Yet even with the restriction to four experiments – $\vec{\text{p}}+\text{p}$, $\vec{\text{p}}+^4$He, $P_\gamma(^{18}\text{F})$, and $A_\gamma(^{19}\text{F})$ – it is clear that all five partial-wave amplitudes contribute to at least one of the observables. Early versions of Fig. 1 arose because it was noted that the observables plotted depended on very similar combinations of DDH isoscalar and isovector couplings – the combination $h^0_\rho+0.7h^0_\omega$ and effectively h^1_π, with very small corrections due to h^1_ρ and h^1_ω. While isotensor PNC contributes to $A_L(\vec{\text{p}}\text{p})$, it plays no role in the other observables. As the purpose of the plot is to determine whether there is consistency among competing experiments, it thus made sense to "freeze out" this degree of freedom. Thus was done by "marginalizing" over the isotensor contribution, allowing it to vary over the DDH reasonable range, while fitting the isoscalar coupling to the measure $A_L(\vec{\text{p}}\text{p})$. This procedure effectively expands the allowed pp band in Fig. 1 – though this expansion is modest because DDH assigned a relatively small reasonable-range uncertainty on h^2_ρ of $\pm 20\%$.

We want to make several observations about Fig 1:

1. The figure shows a region of good overlap between the four experiments. Over most of the last 15 years similar plots showed some tension among the experiments, but it was found recently [5] that this largely originated from the use of inconsistent sets of strong interaction couplings in past analyses. As PNC experimental observables are bilinear in the weak and strong couplings, a fixed set of strong couplings must be used when extracting values of the DDH weak couplings. When the inconsistencies were corrected in

[5], the pp error band move upward, increasing the region of overlap with the results from $\vec{\rm p}$+^{4}He and ^{19}F. This is a welcome development, indicating that patterns are beginning to emerge from experiments.

2. Another motivation for Fig. 1 was to emphasize that certain combinations of weak couplings dominate most observables: thus in some leading-order sense, identifying patterns in hadronic PNC may not require a five-dimensional analyses. EFT approaches provide no guidance on such issues. In contrast, it is clear that certain of the DDH parameters (using their best values as a guide) are more important than others. Unfortunately, one of those parameters is h_π^1 – undercutting any confidence one might have in relying on DDH for establishing the hierarchy of S-P couplings. This raises the question of whether some other theoretical basis exists for considering certain of the LECs as leading, and others as less important, allowing us to focus effort initially on establishing the values of the most important parameters.

3. Fig. 1 is 2D – but the end solution is consistent with $h_\pi^1 \sim 0$. Only one parameter is needed, the isoscalar strength. Had one known this at the start, one might have made another axis choice, using the isoscalar and isotensor directions to define a plane for displaying the experimental results.

Recently there has emerged from large-N_c analyses a way to classify the S-P LECs as either leading or sub-leading. That classification appears to be consistent with the hadronic PNC phenomenology just described, and provides a sound theoretical argument for focusing first on a particular 2D cut through the 3D isoscalar-isotensor volume. In the context of large N_c, the absence of a signal from ^{18}F can be seen as important confirmation of an emerging pattern.

We now describe the new classification of LECs that merges from large-N_c QCD, and how this classification influences our interpretation of existing and anticipated hadronic PNC data.

3 The Large-N_c Classification and Experimental Implications

The lovely large-N_c work of [6, 7] motivates us to pivot in the 5D space of LECs Λ to two new principal axes, one in the 2D $I = 0$ plane and one along the $I = 2$ direction

$$\begin{aligned} \Lambda_0^+ \equiv \frac{3}{4}\Lambda_0^{^3S_1-{}^1P_1} + \frac{1}{4}\Lambda_0^{^1S_0-{}^3P_0} &\sim N_c \\ \Lambda_2^{^1S_0-{}^3P_0} &\sim N_c, \end{aligned} \tag{17}$$

with the remaining three orthogonal axes suppressed in the $1/N_c$ counting

$$\begin{aligned} \Lambda_0^- \equiv \frac{1}{4}\Lambda_0^{^3S_1-{}^1P_1} - \frac{3}{4}\Lambda_0^{^1S_0-{}^3P_0} &\sim 1/N_c \\ \Lambda_1^{^1S_0-{}^3P_0} &\sim \sin^2\theta_w \\ \Lambda_1^{^3S_1-{}^3P_1} &\sim \sin^2\theta_w. \end{aligned} \tag{18}$$

One can consider these three subdominant directions to be N^{2}LO, contributing only in relative order $\sim 1/N_c^2$: this is explicitly the case for the second isoscalar axis, while for the $\Delta I = 1$ amplitudes additional suppression is gained from the weak mixing angle, $\sin^2\theta_w/N_c \sim 12$. Consequently the large-N_c classification may prove to be especially useful in hadronic PNC, with corrections only at the $\sim 10\%$ level.

Table 2 is a large-N_c version of the "Rosetta stone" table of [5]. For the Girlanda coefficients, the key relationships are $\mathcal{G}_1 \sim \tilde{\mathcal{G}}_1 \sim N_c$ and $\mathcal{G}_1 + 2\tilde{\mathcal{G}}_1 \sim 1/N_c$ [7]. The relationships to the

Table 2: A large-N_c hadronic PNC "Rosetta stone": The LECs for the S-P PNC potential of Eq. (7) are organized according to the large-N_c classification of [7]. The relationships to the DDH potential and to the coefficients of Girlanda's EFT potential are shown. Note that multiplicative factor of $2m_N m_\rho^2$ must be applied to the Girlanda entries to obtain the dimensionless coefficients Λ, e.g., $\Lambda_1^{^1S_0-^3P_0} = \mathcal{G}_2$ $[2m_N m_\rho^2]$.

Coeff	DDH	Girlanda	Large N_c
$\Lambda_0^+ \equiv \frac{3}{4}\Lambda_0^{^3S_1-^1P_1} + \frac{1}{4}\Lambda_0^{^1S_0-^3P_0}$	$-g_\rho h_\rho^0(\frac{1}{2}+\frac{5}{2}\chi_\rho) - g_\omega h_\omega^0(\frac{1}{2}\text{-}\frac{1}{2}\chi_\omega)$	$2\mathcal{G}_1 + \tilde{\mathcal{G}}_1$	$\sim N_c$
$\Lambda_0^- \equiv \frac{1}{4}\Lambda_0^{^3S_1-^1P_1} - \frac{3}{4}\Lambda_0^{^1S_0-^3P_0}$	$g_\omega h_\omega^0(\frac{3}{2}+\chi_\omega) + \frac{3}{2}g_\rho h_\rho^0$	$-\mathcal{G}_1 - 2\tilde{\mathcal{G}}_1$	$\sim 1/N_c$
$\Lambda_1^{^1S_0-^3P_0}$	$-g_\rho h_\rho^1(2+\chi_\rho) - g_\omega h_\omega^1(2+\chi_\omega)$	$\mathcal{G}_2$	$\sim \sin^2\theta_w$
$\Lambda_1^{^3S_1-^3P_1}$	$\frac{1}{\sqrt{2}} g_{\pi NN} h_\pi^1 \left(\frac{m_\rho}{m_\pi}\right)^2 + g_\rho(h_\rho^1 - h_\rho^{1\prime}) - g_\omega h_\omega^1$	$2\mathcal{G}_6$	$\sim \sin^2\theta_w$
$\Lambda_2^{^1S_0-^3P_0}$	$-g_\rho h_\rho^2(2+\chi_\rho)$	$-2\sqrt{6}\mathcal{G}_5$	$\sim N_c$

DDH parameters are also shown. On computing DDH best-value equivalents and comparing them to large-N_c expectations, one finds

$$\left\{ \begin{array}{c} {}^{\rm DDH}\Lambda_0^+ \\ {}^{\rm DDH}\Lambda_2^{^1S_0-^3P_0} \end{array} \right\} = \left\{ \begin{array}{c} 319 \\ 151 \end{array} \right\} \qquad \left\{ \begin{array}{c} {}^{\rm DDH}\Lambda_0^- \\ {}^{\rm DDH}\Lambda_1^{^1S_0-^3P_0} \\ {}^{\rm DDH}\Lambda_1^{^3S_1-^3P_1} \end{array} \right\} = \left\{ \begin{array}{c} -70 \\ 21 \\ 1340 \end{array} \right\}, \tag{19}$$

with the LO contributions on the left and the corrections on the right. The units are 10^{-7}. There is a glaring discrepancy in the $\Lambda_1^{^3S_1-^3P_1}$ isovector channel, where the pion contributes. The DDH value for Λ_0^- is also not negligible.

3.1 Experimental constraints on large-N_c LECs

In addition to the above results, we expect to have a new constraint from NPDGamma in hand soon. NPDGamma data taking is finished and the statistical uncertainty of the result has been given as approximately 13 ppb [3]. Current efforts are focused on measuring and subtracting potential systematic effects, including an asymmetry associated with aluminum in the target window. Consequently we express the anticipated asymmetry as

$$|A_\gamma| < \epsilon\, 1.3 \times 10^{-8} \tag{20}$$

under the conservative assumption that the result will be an upper bound (it need not be so) which we set at the statistical uncertainty, while including a parameter $\epsilon > 1$ that will account for consequences of systematic errors, including that associated with the aluminum subtraction. We then find [59, 5] (see also [60, 61])

$$|\Lambda_1^{^3S_1-^3P_1}| < \epsilon\, 270\ . \tag{21}$$

The numerical coefficient provides a measure of the potential impact of the result, given the anticipated statistical error. This bound is important because it is approximately as restrictive as that from $P_\gamma(^{18}\text{F})$, but has a different dependence on the LECs.

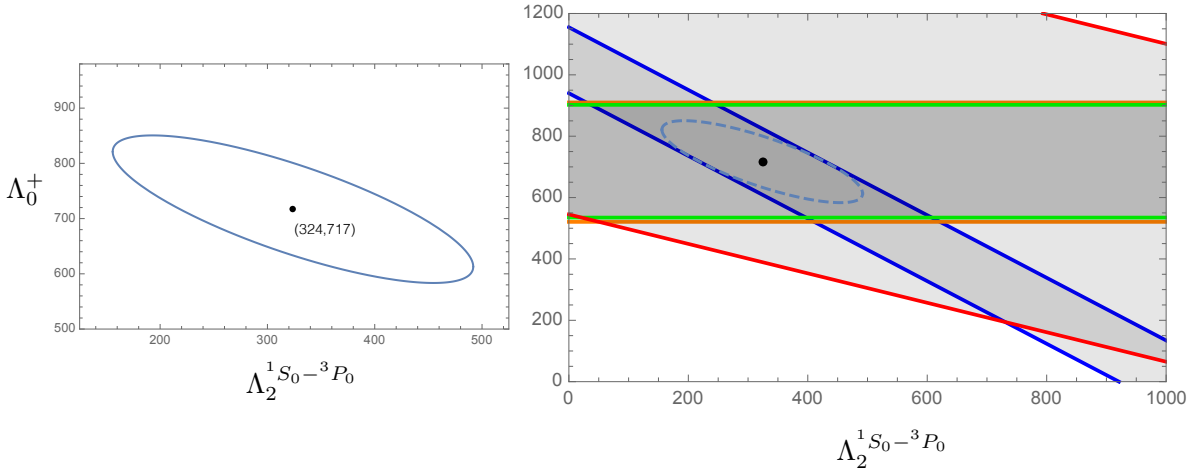

Figure 3: LO large-N_c solutions satisfying all low-energy constraints on hadronic PNC. The left panel provides an expanded view of the region, interior to the ellipse, with $\chi^2 < 1$. The dot marks the best-fit point. On the right the constraints from $A_L(\vec{\mathrm{p}}\mathrm{p})$ at low energies (blue boundary), $A_L(\vec{\mathrm{p}}\mathrm{p})$ at 221 MeV (red), $A_L(\vec{\mathrm{p}}\alpha)$ (orange), and $A_\gamma(^{19}\mathrm{F})$ (green) are shown, along fit the combined allowed region (dashed ellipse). The experimental bands are 1σ. The LECs are given in units of 10^{-7}.

We now express all five results discussed above in the large-N_c LEC basis, sequestering the N^{2}LO terms in brackets

$$\begin{aligned}
\frac{2}{5}\Lambda_0^+ + \frac{1}{\sqrt{6}}\Lambda_2^{^1S_0-^3P_0} + \left[-\frac{6}{5}\Lambda_0^- + \Lambda_1^{^1S_0-^3P_0}\right] &= 419 \pm 43 && A_L(\vec{\mathrm{p}}\mathrm{p}) \\
1.3\Lambda_0^+ + \left[-0.9\Lambda_0^- + 0.89\Lambda_1^{^1S_0-^3P_0} + 0.32\Lambda_1^{^3S_1-^3P_1}\right] &= 930 \pm 253 && A_L(\vec{\mathrm{p}}\alpha) \\
\left[\left|2.42\Lambda_1^{^1S_0-^3P_0} + \Lambda_1^{^3S_1-^3P_1}\right|\right] &< 340 && P_\gamma(^{18}\mathrm{F}) \\
0.92\Lambda_0^+ + \left[-1.03\Lambda_0^- + 0.67\Lambda_1^{^1S_0-^3P_0} + 0.29\Lambda_1^{^3S_1-^3P_1}\right] &= 661 \pm 169 && A_\gamma(^{19}\mathrm{F}) \\
\left[\left|\Lambda_1^{^3S_1-^3P_1}\right|\right] &< \epsilon\, 270 && A_\gamma(\vec{\mathrm{n}}\mathrm{p} \to \mathrm{d}\gamma)
\end{aligned} \quad (22)$$

The LO approximation corresponds to ignoring the bracketed terms while solving the three remaining equations for Λ_0^+ and $\Lambda_2^{^1S_0-^3P_0}$. The best-value solution is $\Lambda_0^+ = 717$ and $\Lambda_2^{^1S_0-^3P_0} = 324$, with a nearly vanishing χ^2 (reflecting the almost exact overlap of the $A_L(\vec{\mathrm{p}}\alpha)$ and $A_\gamma(^{19}\mathrm{F})$ bands). The contour of $\chi^2 = 1$ (the fit has one degree of freedom) encloses the region shown in Fig. 3.

These best values are both more than a factor of two larger than the DDH benchmark values for Λ_0^+ and $\Lambda_2^{^1S_0-^3P_0}$ given in Eq. (19). This indicates that there may be a second shortcoming in Fig. 1, from the perspective of large-N_c QCD: not only were the wrong isospin axes used, but the marginalization that was done to remove the effects of $\Lambda_2^{^1S_0-^3P_0}$ from the band for $A_L(\vec{\mathrm{p}}\mathrm{p})$ likely underestimated the associated uncertainties. In the procedures leading to Fig. 1 it was assumed that the value for h_ρ^2, and consequently $\Lambda_2^{^1S_0-^3P_0}$, would be good to within the estimate reasonable range of $\pm$ 20% around the best value. But the best-value value we found is far outside this band. In fact most of the allowed region for $\Lambda_2^{^1S_0-^3P_0}$ within the ellipse of Fig. 3 would have also been excluded from this band. Consequently it is not surprising that there is a discrepancy between the isoscalar parameter employed in Fig. 1, $-(h_\rho^0 + 0.7h_\omega^0)$, and that associated with Λ_0^+, $-(h_\rho^0 + 0.2h_\omega^0)$.

It is also apparent that there is no evidence for any nonzero contribution from the three N^{2}LO LECs. One way to illustrate this is to solve the three equalities above, turning on just one of the three N^{2}LO LECs, while using the central experimental values. This yields in turn for the three choices

$$\begin{aligned}(\Lambda_0^+, \Lambda_2^{^1S_0-{}^3P_0}, \Lambda_0^-) &= (710, 309, -7)\\ (\Lambda_0^+, \Lambda_2^{^1S_0-{}^3P_0}, \Lambda_1^{^1S_0-{}^3P_0}) &= (667, 199, 71)\\ (\Lambda_0^+, \Lambda_2^{^1S_0-{}^3P_0}, \Lambda_1^{^3S_1-{}^3P_1}) &= (704, 336, 45).\end{aligned}$$

In two cases the result LO parameters do not move outside the $\chi^2 = 1$ ellipse of Fig. 3, showing that any sensitivity to N^{2}LO parameters is buried under experimental noise. As the values of the N^{2}LO parameters are typically comparable to or less than the experimental uncertainties, we conclude that with current data

$$\Lambda_0^- \sim \Lambda_1^{^1S_0-{}^3P_0} \sim \Lambda_1^{^3S_1-{}^3P_1} \sim 0.$$

Thus we do not have the number or quality of results needed to place meaningful constraints on parameters we expect to be $\sim 1/10$ the strength of the LO parameters. This helps to put the NPDGamma effort in context: it represents a heroic effort to make the first measurement of a N^{2}LO LEC.

3.2 The TRIUMF 221 MeV $A_L(\vec{\mathrm{p}}\mathrm{p})$

We noted earlier that the DDH potential is equivalent to an EFT near threshold, and thus can be viewed as a model for extrapolating those results to higher momenta, where ranges controlled by meson masses become important, and where additional degrees of freedom connected with P-D and other high partial wave amplitudes play a role. Conversely, we can work this process in reverse. The two axes of the ellipse in the left panel of Fig. 1 correspond to two constraints, one corresponding to the S-P component of the scattering and the second from the P-D component. The former we have already treated in the analysis of the low-energy data on $A_L(\vec{\mathrm{p}}\mathrm{p})$, but the latter is additional. From the second of Eqs. (32) of [5] we obtain the constraint

$$\Lambda_0^+ + 0.48\Lambda_2^{^1S_0-{}^3P_0} + \left[2.03\Lambda_0^- + 18.8(h_\rho^1 - h_\omega^1)\right] = 1063 \pm 518 \qquad A_L(\vec{\mathrm{p}}\mathrm{p})\big|_{221\ \mathrm{MeV}}\,. \tag{23}$$

Note that a new isovector term arises, expressed in terms of DDH couplings, reflecting the fact that P-D scattering includes new degrees of freedom. For our just determined best values for Λ_0^+ and $\Lambda_2^{^1S_0-{}^3P_0}$, the LO contribution to the left-hand side is 873. There is no evidence for any nonzero N^{2}LO contribution.

3.3 Deconstructing h_π^1: A "$\Delta I = 0$" Rule from Theory and Experiment

We have already noted that there is tension between the values we have found for Λ_0^+ and $\Lambda_2^{^1S_0-{}^3P_0}$ and DDH best values, with the large-N_c LO LECs being about a factor of two large than their DDH analogs. While uncertainties in our fit allow for values of $\Lambda_2^{^1S_0-{}^3P_0}$ as small as the DDH best value, such small values come at the cost of increasing Λ_0^+ even further, as Fig. 3 shows. Thus such an adjustment does not remove the tension.

A even larger discrepancy exists for $\Lambda_1^{^3S_1-{}^3P_1}$, as one can see by comparing the large-N_c predictions of Eqs. (17,18) with that of the DDH best values of Eq. (19). The DDH best value is at least an order of magnitude larger than the naive large-N_c expectation for an N^{2}LO parameter. This is the LEC to which one-pion exchange and thus h_π^1 contributes. The purpose of this section is to describe the likely origin of this mismatch.

Equation (8) shows that the numerical value of ${}^{\rm DDH}\Lambda_1^{{}^3S_1-{}^3P_1}$ is dominated by the pion, as the contribution from vector meson terms is less than 1% of the total. This comes in part because the pion-propagator at low momentum transfers generates a relative enhancement of $(m_\rho^2/m_\pi^2) \sim 30$. This magnifies the pion contribution to the ${}^{\rm DDH}\Lambda_1^{{}^3S_1-{}^3P_1}$ LEC, and also enhances this LEC relative to others. If we compare ${}^{\rm DDH}\Lambda^{{}^3S_1-{}^3P_1}$ to ${}^{\rm DDH}\Lambda_0^+$, no other large, distinguishing factors are found: for example, the DDH best-value effective pion coupling, $g_{\pi{\rm NN}}h_\pi^1/\sqrt{32} \sim 1.08$, is comparable to those appearing in isoscalar channels, $-g_\rho h_\rho^0/2 \sim 1.59$ and $-g_\omega h_\omega^0/2 \sim 0.80$. Thus one is led to the conclusion that a small value for ${}^{\rm DDH}\Lambda_1^{{}^3S_1-{}^3P_1}$ consistent with the large-N_c hierarchy, requires a significant reduction in the DDH best value for h_π^1 – by a factor of 10 or more – to compensate for the propagator enhancement.

The anatomy of the h_π^1 coupling involves both the charged and neutral weak currents. An estimate for the charged current, or "Cabibbo" term, can be based on SU(3)$_f$ symmetry, either with [62, 63, 64, 65] or without [66, 67] the use of PCAC and current algebra techniques. This contribution to the matrix element for $n \to p\pi^-$ can be related to known hyperon decays [63]

$$n_-^0 = -\left(\frac{2}{3}\right)^{1/2}\left[2\Lambda_-^0 - \Xi_-^-\right]\tan\theta_c \equiv g_\pi \ . \tag{24}$$

Recalling that $\tan\theta_c = V_{\rm us}/V_{\rm ud}$ and using the CKM fit of Eq. (12.27) in the CKM review of Ref. [68] we find $\tan\theta_c = 0.231$. Using the experimental values in Table 6.3 of Ref. [69], but the phase conventions of Appendix B in Ref. [10], we find $g_\pi = 0.376 \times 10^{-7}$.

This charged-current contribution can be compared to the "best value" of h_π^1 from Ref. [10], $h_\pi^1 \sim 12 g_\pi$, the value that was used in Eq. (19). The difference reflects in part the neutral current contribution, but also numerical factors associated with the renormalization group (RNG) evolution of the operators of the effective Hamiltonian to the low-momentum scale of interest. There are also SU(3)$_f$ breaking effects to consider. Before discussing these effects explicitly we note that the methods that yield the so-called sum rule estimate of Eq. (24) can also be used to compute n_0^0, the amplitude for $n \to n\pi^0$. In this case, were CP not broken, we should find $n_0^0 = 0$, as first noted by Barton [70]. Indeed this cancellation has been demonstrated explicitly [10], and this serves as a consistency check of the method.

Turning to the balance of the terms in the $\Delta S = 0$ effective weak Hamiltonian, we see, unfortunately, that the methods used in the charged current sector cannot be applied because they rely on the the existence of $(V-A)\times(V-A)$ structures in the weak Hamiltonian. In this case the needed πNN matrix elements have been estimated using an factorization ansatz when possible, supplemented by quark model estimates of the non-factorizable contributions. This, along with an estimate of the leading RNG evolution effects, yields a best estimate of $h_\pi^1 = (0.5 + 11.5)g_\pi = 12 g_\pi$, where the separated factors indicate the charged and neutral current contribution, respectively [10].

However, this analysis has been revisited, particularly by Dubovik and Zenkin [DZ] [36], who extended the three-flavor analysis of DDH to include charm quarks and thus the possibility of GIM cancellation in loop effects [71]. They also evaluate non-factorizable contributions within the MIT bag model. Including operator mixing and RNG evolution, they find a smaller value of $h_\pi^1 \sim 4 g_\pi$, but comparable values of h_ρ^1 and h_ω^1 [36]. The possibility of Δ resonance contributions has been explored by Feldman et al. [37] in the DDH framework, and they have revisited h_π^1 as well, modifying the computation of the factorized contribution as well as that of the strong enhancement associated with the charged-current contribution to find $h_\pi^1 \sim 7 g_\pi$. The updates made by [36] and [37] cannot be easily combined. We regard $h_\pi^1 \sim 1.3 \times 10^{-7}$ [36] as the better estimate.

The computations of h_π^1 we have considered thus far work within a constituent quark model framework, so that operators with strange quarks, albeit with no net strangeness, play no role.

We consider model approaches that can address such operators as well. The possibility of a considerable enhancement within the context of factorization and dimensional analysis has been noted [72]. This issue has been addressed in the Skyrme model. The two-flavor Skyrme model with vector mesons yields a small value of the order of $h_\pi^1 \sim 0.3 \times 10^{-7}$ [73], and thus comparable to g_π. A three-flavor Skyrme model, which can incorporate empirical baryon masses, magnetic moments, and hyperon decays fairly well, has been used to assess the role of four-fermion operators with $(\bar{q}q)(\bar{s}s)$ flavor structure, yielding values for h_π^1 in the range $(0.8 - 1.3) \times 10^{-7}$, considerably larger than the two-flavor result [74]. The authors of Ref. [74] stress that this result is not a consequence of a large (scalar) strangeness component in the nucleon wave function, a notion now in disfavor due to lattice QCD results [75, 76, 77, 78], but rather of operators appearing that involve strange quarks. It is worth noting, however, that the effective PNC Hamiltonian they employ at a scale of ~ 1 GeV includes neither QCD renormalization nor mixing effects in evolving from the weak scale. Such effects would presumably be muted, as noted by DZ [36], by the GIM effects that can arise when the charm quark is included and could lead to additional cancellations. We note that a computation of the low-energy effective Hamiltonian including LO QCD evolution with heavy quarks has been made in the $\theta_c = 0$ limit [79]; this is not a good approximation, however, in the $\Delta I = 1$ sector because the neutral current contribution enters with a factor of $\sin^2\theta_w/3 \simeq 0.08$. For reference the $|\Delta S| = 1$ low-energy effective Hamiltonian, with heavy quarks, has been computed to NLO in QCD [80].

To conclude this section we note that improved assessments of h_π^1 yield results that are considerably smaller than the "best estimate" given by DDH, and are less incompatible with the picture suggested by large N_c and naive dimensional analysis.

The emerging picture points to a dominance of the $\Delta I = 0$ hadronic PNC nucleon amplitudes relative to $\Delta I = 1$ ones, resulting from a combination of the suppression of the latter, and a not insignificant enhancement of the former, relative to DDH best values. This is reminiscent of the dominance of the $\Delta I = 1/2$ amplitude in $K \to \pi\pi$ decay, as was originally pointed out in [19]. We note the recent work of [81, 82].

4 Next Steps

The above arguments show that five significant experimental constraints on hadronic PNC – $A_L(\vec{\mathrm{p}}\mathrm{p})$ near threshold and at 221 MeV, $A_L(\vec{\mathrm{p}}\alpha)$, $P_\gamma(^1\mathrm{F})$, and $A_\gamma(^{19}\mathrm{F})$ – are in excellent accord with expectations arising from large-N_c QCD. In particular, this approach provides two leading-order parameters Λ_0^+ and $\Lambda_2^{^1S_0-{}^3P_0}$ that can be determined from the existing experiments, and appear to account very well for all observations. Three S-P N^{2}LO LECs, expected to be $\sim 10\%$ of the LO LECs, do appear to be small: at least, no existing experiment requires assigning a nonzero value to any of the non-leading LECs. Large N_c thus provides a hierarchical simplification of standard EFT approaches, breaking the five degrees of freedom into a 2+3 pattern. As we have discussed, such a simplification has been tried before, but without sound motivation, leading to descriptions that in hindsight appear flawed. In contrast, the large-N_c hierarchy appears to be sound from the vantage points of both theory and experiment, and particularly useful for hadronic PNC because the correction terms are N^{2}LO, not NLO. The approach provides us with a sensible starting point for planning future work to refine our characterization of the hadronic weak interaction, and thus to understand how this interaction is modified when embedded in strongly interacting systems.

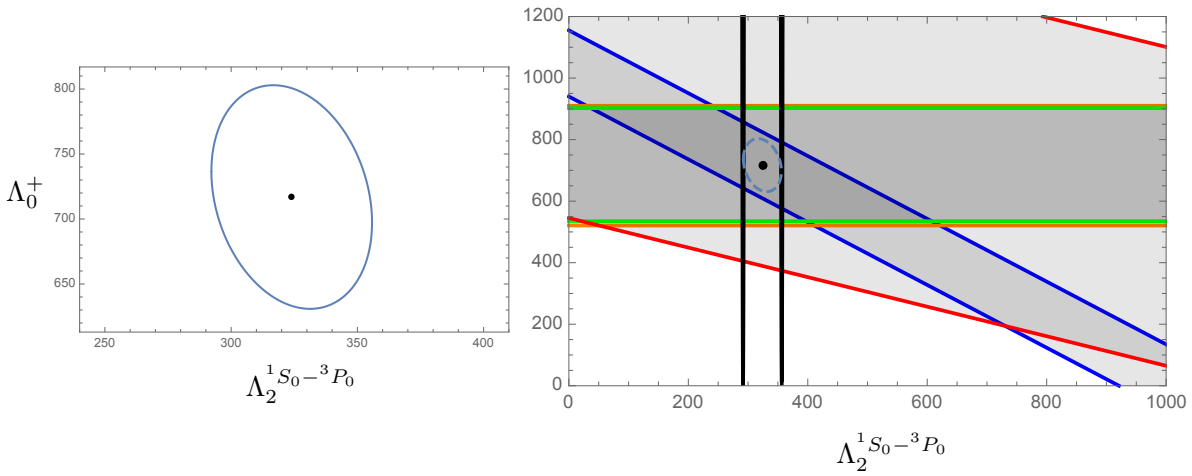

Figure 4: As in Fig. 3, but adding the impact of a future LQCD calculation of the $\Delta I = 2$ amplitude $\Lambda_2^{^1S_0-^3P_0}$ to $\pm$ 10%, centered on the central value from Fig. 3.

4.1 Testing the LO Theory

Despite the quality of the LO fit, there is not a lot of redundancy, especially with the constraints from $A_L(\vec{\mathrm{p}}\alpha)$ and $A_\gamma(^{19}\mathrm{F})$ being so similar. Thus an additional independent measurement sensitive to the LO couplings would be valuable. Furthermore, while the value of $A_L(\vec{\mathrm{p}}\mathrm{p})$ is known to 10%, the errors on the other two experiments exceed 25%. A new measurement matching the precision of $A_L(\vec{\mathrm{p}}\mathrm{p})$, but probing a different combination of Λ_0^+ and $\Lambda_2^{^1S_0-^3P_0}$, thus could substantially shrink the allowed ellipse shown in Fig. 3. A more precise determination of the LO LECs would be important for future searches for N^{2}LO LECs: in experiments where these terms arise in combination with LO terms, even modest errors in LO parameters would obscure the effects of N^{2}LO corrections. There do appear to be opportunities to generate new, high quality constraints on the LO parameters.

Lattice QCD: In lattice QCD (LQCD) one solves strongly interacting problems by replacing the continuum problem with a discretized version, a finite grid in Euclidean space-time with periodic boundary conditions. While this precludes any direct calculation of scattering amplitudes [83], the distortion of the energy levels in a finite volume can be related to low-energy scattering parameters [84, 85, 86] using techniques developed by Lüscher [87, 88]. Most NN scattering calculations documented in the literature were performed with nuclear sources that placed both nucleons at the same space-time point, limiting the results to s-waves. In contrast, applications to hadronic PNC, where p-waves are clearly essential, require the use of extended nuclear sources, placed on the lattice in a variety of configurations that, in sum, allow one to associate lattice eigenvalues with partial waves having good spherical symmetry. This is a nontrivial problem given the cubic symmetry of the lattice. The first calculation of parity-odd two-nucleon scattering using Lüscher's method were recently performed, demonstrating the technique [89].

There is an effort underway to apply LQCD to the problem of calculating $\Lambda_2^{^1S_0-^3P_0}$ [4]. Because this scattering amplitude carries $\Delta I = 2$, there are no disconnected (quark loop) contributions [90]. Thus the statistical noise in this channel should be significantly lower than in $\Delta I = 0, 1$ channels, opening up the possibility of a good LQCD "measurement" near the physical pion mass. A calculation of hadronic PNC in the $\Delta I = 2$ channel is expected to be an order of magnitude less costly than a measurement in the $\Delta I = 1$ channel. Preliminary

work on $\Delta I = 2$ NN PN yielded a non-zero signal [4], and led to the identification of improved interpolating operators, significantly reducing the contamination from nucleon excited states at early times, at least for the heavy pion masses ($m_\pi \sim 700$ and ~ 800 MeV) that were used in these exploratory calculations. Phenomenologically relevant calculations will likely require calculations with $m_\pi \lesssim 300$ MeV, where valid comparisons can be made to low-energy EFTs [91, 92, 93, 94, 95, 96].

The gestation period for major experiments in hadronic PNC, such as NPDGamma, can approach a decade or more. Recent improvements in LQCD applications to NN interactions have been rapid, and the basic tools are in place for a major attack on $\Lambda_2^{^1S_0-^3P_0}$. Thus LQCD might turn out to be the fastest route to determining $\Lambda_2^{^1S_0-^3P_0}$ to the desired precision of 10%. The impact of such a result, illustrated in Fig. 4, would be quite significant.

There was an early, exploratory calculation of h_π^1 in lattice QCD by Wasem, at $m_\pi \sim 389$ MeV [40]. Instead of an NN amplitude, a three-point function [97] corresponding to a nucleon-to-resonance transition through pion absorption was calculated. The calculation did not include nonperturbative renormalization of the bare PNC operators, a chiral extrapolation to the physical pion mass, or the contributions from disconnected (quark loop) diagrams. The result obtained, $h_\pi^1 = (1.10 \pm 0.51 \pm 0.06)^{-7}$, is consistent with the ^{18}F upper bound $|h_\pi^1| \lesssim 1.3 \times 10^{-7}$. The recent developments describe above, for direct calculations of NN PNC amplitudes, now supersede this approach.

New experiments constraining LO LECs: While one could envision developing new experiments to complement existing measurements on $A_L(\vec{\mathrm{p}}\mathrm{p})$, it strikes us that the most conservative strategy might be to re-examine previous efforts on $A_L(\vec{\mathrm{p}}\alpha)$ and $A_\gamma(^{19}\mathrm{F})$, to see if improvements are possible. Specifically, our analysis uses results from the 1985 measurement of $A_L(\vec{\mathrm{p}}\alpha) = (-3.34 \pm 0.9) \times 10^{-7}$ from Lang et al. [49], which was performed with a 1.3 μA polarized beam from the Swiss Institute for Nuclear Research cyclotron. The beam's polarization was switched at the ion source every 30 msec. The experiment utilized techniques that the group had developed in its earlier $A_L(\vec{\mathrm{p}}\mathrm{p})$ experiment [44, 45, 46], to control systematics. If the 1σ error bar on this result could be reduced by a factor ~ 2.5, the desired precision of $\sim 10\%$ would be reached.

From the error budget provided, and assuming that the statistical and systematic errors were added in quadrature in forming the final result, it appears that the statistical contribution is somewhat larger. Thus an experiment delivering about an order of magnitude more beam on target, combined with a reduction in the systematic error of about a factor of two, could be required. The latter will be challenging: the PSI group worked very hard to measure and correct for residual transverse components in the polarized beam, induced by nonuniform magnetic fields in the cyclotron. This was the principal systematic. Thus a new experiment would need to do even better. Nevertheless, it strikes us that an approach such as this that builds on past experience, with a proven technology and with sources of systematic error well documented – could be preferable to starting an effort that lacks such a history.

The few-body theory used to relate the measurements to NN S-P amplitudes should also be updated: there are several modern techniques that could be applied to this problem, including quantum Monte Carlo [98].

Alternatively, one could consider a new attempt on $A_\gamma(^{19}\mathrm{F})$, one of two cases where axial charge β decay is available as a nuclear matrix element calibration. One important aspect of this experiment is the success in controlling systematic errors: The analysis of [51] found that systematic errors were negligible, contributing to the overall uncertainty at a level that would have allowed a 10% measurement, had the statistics been available. Thus a repetition of this experiment with a factor of 20 increase in counting could reach the target 10% uncertainty. As

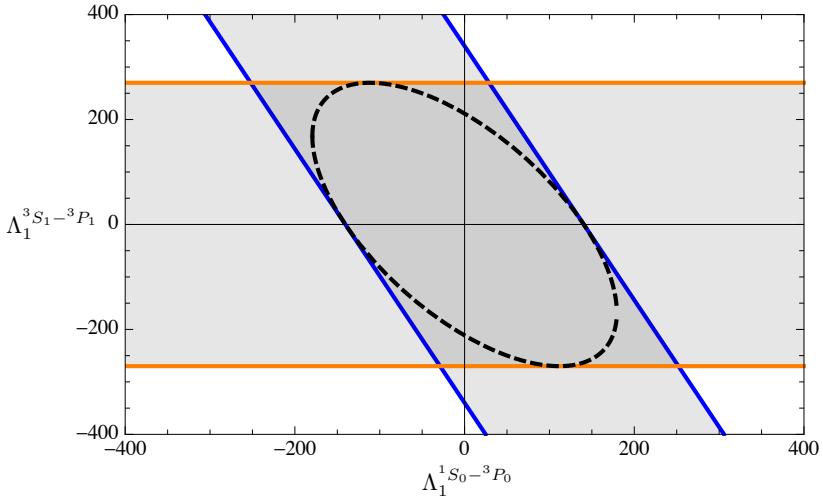

Figure 5: The progress in constraining the large-N_c isovector N^{2}LO LECs that will result from combining anticipated NPDGamma results (horizontal band) with the existing constraint from $P_\gamma(^{18}\mathrm{F})$ (vertical band). The former assumes a central value of zero for $A_\gamma(\vec{\mathrm{n}}\mathrm{p} \to \mathrm{d}\gamma)$ and an uncertainty determined by the experiment's statistics, and thus assumes that the current campaign to subtract out window-induced asymmetries will yield a final systematic uncertainty well below the statistical uncertainty. Note that both isovector LECs are bounded once NPDGamma results are combined with $P_\gamma(^{18}\mathrm{F})$, while neither is bounded without this result. The LECs are in units of 10^{-7}.

^{19}F was produced using a relatively modest 0.4 μA 5 MeV polarized proton beam, the needed statistics might be attainable.

4.2 Testing the N^{2}LO Theory: NPDGamma and $P_\gamma(^{18}\mathrm{F})$

A significant outcome of our work is the recognition that 1) past experiments have done a good job in characterizing the LO large-N_c interaction – with further improvements possible in the near term, such as that illustrated in Fig. 4 – and 2) we have already embarked on a credible campaign to learn about the N^{2}LO corrections. From the perspective of this second point, the striking aspect of Eqs. (22) is that $\Lambda_1^{^1S_0-{}^3P_0}$ and and $\Lambda_1^{^3S_1-{}^3P_1}$ are the low-hanging fruit in this endeavor, because we can use isospin to restrict ourselves to the $\Delta I = 1$ plane in our 5D parameter space, where no LO terms exist to mask the smaller effects we seek. Furthermore, we have already embarked on a nearly optimal program to limit or measure these parameters, with $P_\gamma(^{18}\mathrm{F})$ and NPDGamma being ideal choices for this task.

An important question to ask is where we might stand, once NPDGamma announces its result. To assess this we make the choice $\epsilon \sim 1$, which is a possible outcome as the important systematic effects in the experiment appear to be isolated in the window subtraction, including Al as the dominant correction. The net results that would follow from combining the bound on $P_\gamma(^{18}\mathrm{F})$ with a NPDGamma $A_\gamma(\vec{\mathrm{n}}\mathrm{p} \to \mathrm{d}\gamma)$ result centered on zero with a final error bar of 1.3×10^{-8} is shown in Fig. 5. Note that a central value for A_γ other than zero would shift the horizontal band up or down, while significant residual systematic uncertainties leading to $\epsilon > 1$ would broaden the band proportionately. One observes that the two experiments are very complementary, probing different combinations of the two $\Delta I = 1$ LECs. If one uses $\Lambda_0^+ \sim 700$ as the scale of the LO contribution, then current $P_\gamma(^{18})\mathrm{F}$ and potential NPDGamma constraints are about a factor of three below the LO scale, or roughly at the NLO level. Thus considerable work remains ahead, as these constraints should be improved another factor of

three, if the LECs are of natural size.

Figure 5 also shows that the NPDGamma result is essential in placing such bounds on $\Lambda_1^{^1S_0-{}^3P_0}$ and $\Lambda_1^{^3S_1-{}^3P_1}$: $P_\gamma(^{18}\mathrm{F})$ by itself constrains neither to be below the LO scale. The two measurements are highly complementary, testing distinct combinations of the $\Delta I = 1$ LECs.

Next-generation experiments to reach the N^{2}LO level will be challenging, and would be more easily motivated if the needed sensitivity to see N^{2}LO contributions could be better defined. If current LQCD efforts to determine $\Lambda_2^{^1S_0-{}^3P_0}$ at the 10% level meet with success, then the N^{2}LO contributions might be the next LQCD challenge. While the presence of disconnected diagrams would substantially increase the difficulty of $\Delta I = 1$ calculations, the detection of a signal of any quality would be helpful to the field, potentially confirming the predicted large-N_c coupling hierarchy and providing a definite target for the experimentalists.

4.3 The potential impact of new experiments

Several recent proposals have been made to initiate new experiments, and others have been pursued or discussed in the past. The large-N_c LEC hierarchy can be used to determine how new experiments will impact our understanding of hadronic PNC. We first describe some of the potential observables:

a) An effort to measure the longitudinal asymmetry for scattering polarized neutrons from a ^{3}He target – $\vec{n} + {}^3\mathrm{He} \to {}^3\mathrm{H} + p$ – is underway at the SNS. The predicted value, based on calculations by Viviani et al. using the AV18 potential with the UIX three-body interaction is [99]

$$\frac{364}{10^{-8}}\, A_\mathrm{p} = -\Lambda_0^+ + 0.227\Lambda_2^{^1S_0-{}^3P_0} - \left[3.82\Lambda_0^- + 8.18\Lambda_1^{^1S_0-{}^3P_0} + 2.27\Lambda_1^{^3S_1-{}^3P_1}\right] . \quad (25)$$

Using the best-fit parameters for the two LO LECs yields $A_\mathrm{p} \sim -1.8 \times 10^{-8}$. As the relative sign of the two LO LECs is opposite to that found for $A_L(\vec{\mathrm{p}}\mathrm{p})$, a measurement of a nonzero value would generate a complementary band in Fig. 3, testing the region of intersection identified there.

b) There was a past attempt to detect the gamma ray asymmetry produced when longitudinally polarized neutrons capture on a deuterium target, $\vec{\mathrm{n}} + \mathrm{d} \to \mathrm{t} + \gamma$. $A_\gamma(\vec{\mathrm{n}}\mathrm{d})$ is a rare example of a few-nucleon PNC observable where some enhancement occurs, as the parity-conserving M1 amplitude is suppressed at thermal neutron energies. The predicted asymmetry is [100]

$$\frac{118}{10^{-7}}\, A_\gamma = \Lambda_0^+ + 0.44\Lambda_2^{^1S_0-{}^3P_0} - \left[1.86\Lambda_0^- + 0.65\Lambda_1^{^1S_0-{}^3P_0} + 0.42\Lambda_1^{^3S_1-{}^3P_1}\right], \quad (26)$$

yielding $\sim 7.3 \times 10^{-7}$ for the LO best values. The value obtained in an experiment by Avenier et al. [58], $\sim 8 \times 10^{-6}$, is an order of magnitude larger. This result has been largely ignored because of concerns about unidentified systematics [19].

c) There are several np observables complementary to NPDGamma's $A_\gamma(\vec{\mathrm{n}}\mathrm{p})$. Significant effort has been invested in studies of the circular polarization of the 2.2 MeV gamma ray produced in thermal neutron capture on the proton. The circular polarization [59],

$$\frac{825}{10^{-7}}\, P_\gamma = \Lambda_0^+ + 1.27\Lambda_2^{^1S_0-{}^3P_0} + \left[0.47\Lambda_0^-\right], \quad (27)$$

is $\sim 1.4 \times 10^{-7}$ for the LO LEC best values. The combination of three separate measurements and various control experiment by Knyaz'kov et al. led to a determination

$P_\gamma = (1.8 \pm 1.8) \times 10^{-7}$ [57], superseding an earlier result that apparently was contaminated by bremmstrahlung from the reactor core [101]. Recently interest has been expressed in measuring the inverse reaction, the circular polarization dependence of the breakup reaction $\vec{\gamma} d \to \mathrm{n} + \mathrm{p}$, which of course has an identical dependence on the LECs. This has been proposed as a commissioning experiment at at upgraded Hiγs facility [102]

d) The neutron spin rotation of polarized cold neutrons traversing a parahydrogen target is a third possible np observable. The experiment is feasible because strong interaction spin-flip scattering off parahydrogen (S=0 molecules) is forbidden. The spin rotation, taken from the Paris potential results of [103] as modified by [104, 105] (see also [106, 60, 107]),

$$\frac{180}{10^{-7}} \frac{d\phi^{\mathrm{n}}}{dz}\Big|_{\mathrm{parahydrogen}} = \left(\Lambda_0^+ + 2.82\Lambda_2^{{}^1S_0-{}^3P_0} - \left[3.15\Lambda_0^- + 1.94\Lambda_1^{{}^3S_1-{}^3P_1}\right]\right) \text{ rad/m}, \quad (28)$$

is $\sim 9.1 \times 10^{-7}$ rad/m for the best-value LO LECs. To date there has been no experiment mounted. This is also the case with a fourth possible np observable, the dependence of the capture cross section on the neutron helicity, which tests a combination of LECs identical to that appearing above. Note that the neutron spin rotation in deuterium has also been calculated [108].

e) A neutron spin rotation experiment has been attempted in He, where from [109],

$$\frac{105}{10^{-7}} \frac{d\phi^{\mathrm{n}}}{dz}\Big|_{{}^4\mathrm{He}} = \left(\Lambda_0^+ - \left[1.61\Lambda_0^- + 0.92\Lambda_1^{{}^1S_0-{}^3P_0} + 0.35\Lambda_1^{{}^3S_1-{}^3P_1}\right]\right) \text{ rad/m} \quad (29)$$

which leads to a predicted LO spin rotation of 6.8×10^{-7} rad/m. The experiment, performed on the slow neutron beam line at NIST, established the upper bound $(1.7 \pm 9.1 \pm 1.4) \times 10^{-7}$ [56].

f) The longitudinal analyzing power for the scattering of polarized protons on deuterium, where [110]

$$\frac{156}{10^{-8}} A_L = -\Lambda_0^+ + \left[1.75\Lambda_0^- - 1.09\Lambda_1^{{}^1S_0-{}^3P_0} - 1.25\Lambda_1^{{}^3S_1-{}^3P_1}\right], \quad (30)$$

leading to a LO large-N_c estimate of $A_L = -4.6 \times 10^{-8}$. An experiment was done at 15 MeV nearly 40 years ago, yielding the result $A_L = (-3.5 \pm 8.5) \times 10^{-8}$ [43].

A summary of this discussion is presented in Table 3. All of the above experiments belong in the same class as those displayed in Fig. 3, presumably dominated by the LO LECs. Thus it would be appropriate to set goals, for future efforts on these observables, that will guarantee they improve the pattern in that figure. To be competitive, uncertainties should then be achieved that are at least comparable to those of the $A_L(\vec{p}\alpha)$ and $A_\gamma(^{19}\mathrm{F})$ measurements, which as noted previously are $\sim 25\%$. The last two experiments in the table are only sensitive to Λ_0^+, and thus can be viewed as surrogates for $A_L(\vec{p}\alpha)$ and $A_\gamma(^{19}\mathrm{F})$. As we have argued that it is important to reduce the errors on these measurements to $\sim 10\%$, better defining the two LO LECs, one might consider whether that goal could be reached more easily via $A_L(\vec{\mathrm{p}}\mathrm{d})$ or neutron spin rotation in ^{4}He.

Four of the experiments depend on linear combinations of Λ_0^+ and $\Lambda_2^{{}^1S_0-{}^3P_0}$, and in three cases these combinations are not too different from that tested in $A_L(\vec{\mathrm{p}}\mathrm{p})$. Consequently not a lot will be learned unless a $\sim 10\%$ uncertainty comparable to that of $A_L(\vec{\mathrm{p}}\mathrm{p})$ is achieved. The observable $A_{\mathrm{p}}(\vec{\mathrm{n}}+{}^3\mathrm{He} \to {}^3\mathrm{H}+\mathrm{p})$, which is the subject of an ongoing experiment [1], is notable because the contributions from Λ_0^+ and $\Lambda_2^{{}^1S_0-{}^3P_0}$ carry opposite signs. A high quality result

Table 3: Candidate future hadronic PNC experiments, including several that have been or are now being pursued. The LO large-N_c estimates for the observables are given, along with the functional dependence on the LECs.

Observable	Exp. Status	LO Expectation	LO LEC Dependence
$A_{\rm p}(\vec{\rm n}+^3{\rm He}\to{}^3{\rm H}+{\rm p})$	ongoing	-1.8×10^{-8}	$-\Lambda_0^+ + 0.227\Lambda_2^{^1S_0-{}^3P_0}$
$A_\gamma(\vec{\rm n}+{\rm d}\to{\rm t}+\gamma)$	8×10^{-6} (see text) [58]	7.3×10^{-7}	$\Lambda_0^+ + 0.44\Lambda_2^{^1S_0-{}^3P_0}$
$P_\gamma({\rm n}+{\rm p}\to{\rm d}+\gamma)$	$(1.8\pm1.8)\times10^{-7}$ [57]	1.4×10^{-7}	$\Lambda_0^+ + 1.27\Lambda_2^{^1S_0-{}^3P_0}$
$\frac{d\phi^{\rm n}}{dz}\big\vert_{\rm parahydrogen}$	none	9.4×10^{-7} rad/m	$\Lambda_0^+ + 2.7\Lambda_2^{^1S_0-{}^3P_0}$
$\frac{d\phi^{\rm n}}{dz}\big\vert_{^4{\rm He}}$	$(1.7\pm9.1\pm1.4)\times10^{-7}$ [56]	6.8×10^{-7} rad/m	Λ_0^+
$A_L(\vec{\rm p}+{\rm d})$	$(-3.5\pm8.5)\times10^{-8}$ [43]	-4.6×10^{-8}	$-\Lambda_0^+$

would place a fifth band on Fig. 3, oblique to those now there. That would very helpful in testing the large-N_c picture. An uncertainty on $A_{\rm p}(\vec{\rm n}+^3{\rm He}\to{}^3{\rm H}+{\rm p})$ of $\lesssim 0.5\times10^{-8}$ would have a major impact on Fig 3.

All of these remarks are made under the assumption that N^{2}LO corrections are indeed of the naively expected size, $\sim 10\%$. If this assumption is wrong, then the question of the role of candidate new experiments becomes more complicated. We also remark that none of the experiments in Table 3 is like ^{18}F and NPDGamma, exclusively sensitive to N^{2}LO corrections. This underscores how important these two experiments are, providing a unique opportunity to establish the scales of two of the three N^{2}LO LEC cleanly, and thus to verify the predicted large-N_c LEC hierarchy.

5 Summary and Outlook

The field of hadronic PNC began three score years ago, when it was recognized that the weak semileptonic interaction responsible for nuclear beta decay violates parity and that there should exist a corresponding parity-violating signal in the NN interaction due to the nonleptonic weak force. By exploiting the parity violation, it was realized one could isolate this interaction despite its embedding in a strongly interacting system, testing our understanding of W- and Z-exchange among the quarks. NN and nuclear systems were recognized as uniquely important to the study of the neutral current, which plays no role in strangeness-changing interactions due to the absence of flavor-changing neutral currents. For many years it has been anticipated that the neutral current would be revealed in a PNC $\Delta I = 1$ interaction of long range, generated by pion exchange. The expectation that this interaction would have important consequences for PNC observables has influenced PNC analyses since the 1980s. Yet, the combination of experimental data, large-N_c arguments, and subsequent re-examinations of QCD effects influencing the size of h_π^1, today all indicate otherwise.

Experimental progress in this field has been slow due to the difficulty of measuring effects with a natural size of order $(Gm_\pi^2) \sim 10^{-7}$ relative to the strong interaction: despite the distinctive character of PNC observables, there are many systematics that can lead to false signals at this level. On the theoretical side one had the challenge of five independent S-P

Danilov amplitudes, and very few measurements to constrain these amplitudes. There was a need to find some organizing principle to simplify this task. Influenced by meson-exchange models of PNC, the interest in the $\Delta I = 1$ interaction, and the absence of $\Delta I = 2$ contributions to the data displayed in Fig. 3 (apart from $A_L(\vec{\mathrm{p}}\mathrm{p})$), the choice was made to focus on average $\Delta I = 0$ and 1 strengths, reducing the S-P interaction to two effective couplings. Compounded by some inconsistent treatments of couplings, resolved only recently [5], this led to a puzzling pattern, including the conclusion that the $\Delta I = 1$ degree of freedom was unneeded.

Meson exchange models like the DDH potential attempt to predict weak couplings, a daunting task given the uncertainties inherent in embedding weak interactions in a strongly interacting environment. Beginning about 10 years ago, pionless effective field theories began to be employed. As we have noted in this article, this approach is closely related to the Danilov amplitudes and to the contact potential of Desplanques and Missimer, which date to the field's early days. Furthermore the DDH potential is operationally identical to pionless EFT, in the S-P limit. Thus it could be argued there is little new in the EFT approach. On the other hand, EFT forces one to again confront the issue of five independent S-P amplitudes: there is no organizational principle in EFT for reducing the number of LECs to a more manageable number. The LECs appear as equivalent constants that must be determined from experiment.

This is why the recent application of large-N_c to the PNC is such an important step forward: it provides a hierarchical division of the LECs into two groups, two LO LEC with $\Delta I = 0$ and $\Delta I = 2$, and three N^{2}LO LECs that naively are $\sim 10\%$ corrections, two of which carry $\Delta I = 1$ and one $\Delta I = 0$. The purpose of this review has been to apply this formalism to the full body of information available on PNC. The LO LECs – Λ_0^+ and $\Lambda_2^{^1S_0-{}^3P_0}$ – can be reasonably well determined from existing PNC results, and the resulting LO large-N_c effective theory accounts for all of the existing measurements. We have also argued that the remaining three constants—$\Lambda_1^{^1S_0-{}^3P_0}$, $\Lambda_1^{^3S_1-{}^3P_1}$, and Λ_0^- – do indeed contribute at a suppressed level. More precisely, if NPDGamma produces a result close to its announced statistical precision, it can be combined with $P_\gamma(^{18}\mathrm{F})$ to constrain $\Lambda_1^{^1S_0-{}^3P_0}$ and $\Lambda_1^{^3S_1-{}^3P_1}$ to values considerably below that of Λ_0^+.

In retrospect, the field has been very fortunate in its choice of experiments. $A_L(\vec{\mathrm{p}}\mathrm{p})$, $A_L(\vec{\mathrm{p}}\alpha)$, and $A_\gamma(^{19}\mathrm{F})$ have allowed us to extract the large-N_c LO LECs. $P_\gamma(^{18}\mathrm{F})$ and $A_\gamma(\vec{\mathrm{n}}\mathrm{p} \to \mathrm{d}\gamma)$ probe the N^{2}LO $\Delta I = 1$ plane in complementary ways, potentially allowing us to demonstrate the LEC hierarchy suggested by large N_c by constraining two of the subdominant LECs.

It strikes us that, after many years during which the theoretical and experimental situations were less clear, we are beginning to understand the pattern of PNC in NN systems. There are opportunities to make further progress – to pick experiments that optimally constrain the LECs and test the patterns predicted by large N_c. These include

i) A lattice QCD evaluation of the couplings, beginning with measurement of the $\Delta I = 2$ parameter $\Lambda_2^{^1S_0-{}^3P_0}$. A measurement accurate to 10% would significant narrow the uncertainties on Λ_0^+ and $\Lambda_2^{^1S_0-{}^3P_0}$. This calculation is the natural first step for LQCD, as the $\Delta I = 2$ amplitude has no contributions from disconnected (quark loop) diagrams.

ii) An improved determination of the LO parameters Λ_0^+ and $\Lambda_2^{^1S_0-{}^3P_0}$ by a modern and higher precision measurement of the $\vec{p}\alpha$ longitudinal analyzing power and/or the ^{19}F photon decay asymmetry.

iii) Alternatively, an improved determination of the LO parameters Λ_0^+ and $\Lambda_2^{^1S_0-{}^3P_0}$ by one of the new experiments listed in Table 3. We have noted that $A_L(\vec{n} + {}^3\mathrm{He} \to {}^3\mathrm{H} + p)$ would be a particularly good choice.

iv) A test of the N^{2}LO parameters $\Lambda_1^{^1S_0-^3P_0}$, $\Lambda_1^{^3S_1-^3P_1}$, and Λ_0^- by a modern and higher precision ^{18}F circular polarization measurement and/or a second-generation $\vec{n}p \to d\gamma$ experiment that limits statistical and systematic errors to $\lesssim 0.5 \times 10^{-8}$.

Undertaking all or some combination of these efforts could confirm the large-N_c picture outlined and provide accurate values for four of its five LECs. This in turn could finally demonstrate that the six-decade-long program to understand hadronic PNC has been successful.

Acknowledgements

The authors acknowledge the hospitality of the Kavli Institute for Theoretical Physics and NSF support under award PHY11-25915. The work of SG was supported by the Department of Energy under award DE-FG02-96ER40989, while that of WCH was supported by the Department of Energy under awards de-sc00046548, DE-AC02-98CH10886, and KB0301052 and by the Simons Foundation.

References

[1] C. Crawford, "A new era in discrete hadronic symmetries," 2016. http://online.kitp.ucsb.edu/online/nuclear-c16/ .

[2] J. Fry *et al.*, "Status of the NPDGamma experiment," *Hyperfine Interact.* **238** no. 1, (2017) 11.

[3] J. Fry *et al.*, "Status of the NPDGamma analysis," 2015. http://meetings.aps.org/link/BAPS.2015.APR.S6.2 .

[4] T. Kurth, E. Berkowitz, E. Rinaldi, P. Vranas, A. Nicholson, M. Strother, A. Walker-Loud, and E. Rinaldi, "Nuclear parity violation from lattice QCD," *PoS* **LATTICE2015** (2016) 329, arXiv:1511.02260 [hep-lat].

[5] W. Haxton and B. Holstein, "Hadronic parity violation," *Prog. Part. Nucl. Phys.* **71** (2013) 185–203, arXiv:1303.4132 [nucl-th].

[6] D. R. Phillips, D. Samart, and C. Schat, "Parity-violating nucleon-nucleon force in the $1/N_c$ Expansion," *Phys. Rev. Lett.* **114** no. 6, (2015) 062301, arXiv:1410.1157 [nucl-th].

[7] M. R. Schindler, R. P. Springer, and J. Vanasse, "Large-N_c limit reduces the number of independent few-body parity-violating low-energy constants in pionless effective field theory," *Phys. Rev.* **C93** no. 2, (2016) 025502, arXiv:1510.07598 [nucl-th].

[8] J. F. Donoghue, E. Golowich, and B. R. Holstein, "Dynamics of the standard model," *Camb. Monogr. Part. Phys. Nucl. Phys. Cosmol.* **2** (1992) 1–540. [Camb. Monogr. Part. Phys. Nucl. Phys. Cosmol.35(2014)].

[9] L. Maiani, "Universality of the Weak Interactions, Cabibbo theory and where they led us," *Riv. Nuovo Cim.* **34** (2011) 679–692, arXiv:1303.5000 [hep-ph].

[10] B. Desplanques, J. F. Donoghue, and B. R. Holstein, "Unified treatment of the parity violating nuclear force," *Annals Phys.* **124** (1980) 449.

[11] C. Barnes, M. Lowry, J. Davidson, R. Marrs, F. Morinigo, *et al.*, "Search for neutral weak current effects in the nucleus F-18," *Phys. Rev. Lett.* **40** (1978) 840–843.

[12] P. G. Bizetti *et al.*, "Search for parity mixing in ^{18}F," *Lett. Nuovo Cimento* **29** (1980) 167.

[13] G. Ahrens, W. Harfst, J. Kass, E. Mason, H. Schober, G. Steffens, H. Waeffler, P. Bock, and K. Grotz, "Search for parity violation in the 1081 keV gamma transition of ^{18}F," *Nucl. Phys.* **A390** (1982) 486–508.

[14] M. Bini, T. Fazzini, G. Poggi, and N. Taccetti, "Search for the circular polarization of the 1081-keV gamma ray in F-18," *Phys. Rev. Lett.* **55** (1985) 795–798.

[15] S. Page, H. Evans, G. Ewan, S. Kwan, J. Leslie, *et al.*, "Weak pion-nucleon coupling strength: New constraint from parity mixing in ^{18}F," *Phys. Rev.* **C35** (1987) 1119–1131.

[16] W. Haxton, "Parity nonconservation in ^{18}F and meson exchange contributions to the axial charge operator," *Phys. Rev. Lett.* **46** (1981) 698.

[17] C. Bennett, M. M. Lowrey, and K. Krien, *Bull. Am. Phys. Soc.* **25** (1980) 486.

[18] E. Adelberger, M. Hindi, C. Hoyle, H. Swanson, R. Von Lintig, *et al.*, "Beta decays of Ne-18 and Ne-19 and their relation to parity mixing in F-18 and F-19," *Phys. Rev.* **C27** (1983) 2833–2856.

[19] E. G. Adelberger and W. C. Haxton, "Parity violation in the nucleon-nucleon Interaction," *Ann. Rev. Nucl. Part. Sci.* **35** (1985) 501–558.

[20] M. Gericke, R. Alarcon, S. Balascuta, L. Barron-Palos, C. Blessinger, *et al.*, "Measurement of parity-violating gamma-ray asymmetry in the capture of polarized cold neutrons on protons," *Phys. Rev.* **C83** (2011) 015505.

[21] S. A. Page *et al.*, "Measurement of parity violation in np capture: the NPDGamma experiment," *J. Res. Natl. Inst. Stand. Technol.* **110** (2005) 195–204.

[22] C. Crawford, "The NPDGamma experiment at the SNS FnPB," 2007. http://meetings.aps.org/link/BAPS.2007.DNP.CD.5 .

[23] S.-L. Zhu, C. Maekawa, B. Holstein, M. Ramsey-Musolf, and U. van Kolck, "Nuclear parity-violation in effective field theory," *Nucl. Phys.* **A748** (2005) 435–498, `arXiv:nucl-th/0407087 [nucl-th]`.

[24] L. Girlanda, "On a redundancy in the parity-violating 2-nucleon contact Lagrangian," *Phys. Rev.* **C77** (2008) 067001, `arXiv:0804.0772 [nucl-th]`.

[25] D. R. Phillips, M. R. Schindler, and R. P. Springer, "An effective-field-theory analysis of low-energy parity-violation in nucleon-nucleon scattering," *Nucl. Phys.* **A822** (2009) 1–19, `arXiv:0812.2073 [nucl-th]`.

[26] G. Danilov, "Circular polarization of γ quanta in absorption of neutrons by protons and isotopic structure of weak interactions," *Phys. Lett.* **18** (1965) 40–41.

[27] G. Danilov, "Dispersion approach to the investigation of the weak nucleon-nucleon interaction," *Phys. Lett.* **B35** (1971) 579–580.

[28] G. S. Danilov, *Sov. J. Nucl. Phys.* **14** (1972) 443.

[29] T. D. Lee and C.-N. Yang, "Question of parity conservation in weak Interactions," *Phys. Rev.* **104** (1956) 254–258.

[30] C. S. Wu, E. Ambler, R. W. Hayward, D. D. Hoppes, and R. P. Hudson, "Experimental test of parity conservation in beta decay," *Phys. Rev.* **105** (1957) 1413–1414.

[31] N. Tanner, "Parity in nuclear reactions," *Phys. Rev.* **107** (1957) 1203–1204.

[32] W. Haeberli and B. R. Holstein, "Parity violation and the nucleon-nucleon system," `arXiv:nucl-th/9510062 [nucl-th]`.

[33] M. J. Ramsey-Musolf and S. A. Page, "Hadronic parity violation: A new view through the looking glass," *Ann. Rev. Nucl. Part. Sci.* **56** (2006) 1–52, `arXiv:hep-ph/0601127 [hep-ph]`.

[34] K. Krane, C. Olsen, J. R. Sites, and W. Steyert, "Observation of 1.5% parity-nonconserving gamma-ray asymmetry," *Phys. Rev. Lett.* **26** (1971) 1579–1581.

[35] V. Yuan, C. Bowman, J. Bowman, J. E. Bush, P. Delheij, *et al.*, "Parity nonconservation in polarized-neutron transmission through La-139," *Phys. Rev.* **C44** (1991) 2187–2194.

[36] V. M. Dubovik and S. V. Zenkin, "Formation of parity nonconserving nuclear forces in the standard model SU(2)(l) X U(1) X SU(3)(c)," *Annals Phys.* **172** (1986) 100–135.

[37] G. B. Feldman, G. A. Crawford, J. Dubach, and B. R. Holstein, "Delta contributions to the parity violating nuclear interaction," *Phys. Rev.* **C43** (1991) 863–874.

[38] M. Schindler and R. Springer, "The theory of parity violation in few-nucleon systems," *Prog. Part. Nucl. Phys.* **72** (2013) 1–43, `arXiv:1305.4190 [nucl-th]`.

[39] B. Desplanques and J. H. Missimer, "An analysis of parity violating nuclear effects at low energy," *Nucl. Phys.* **A300** (1978) 286–312.

[40] J. Wasem, "Lattice QCD calculation of nuclear parity violation," *Phys. Rev.* **C85** (2012) 022501, `arXiv:1108.1151 [hep-lat]`.

[41] J. Carlson, R. Schiavilla, V. Brown, and B. Gibson, "Parity violating interaction effects 1: The longitudinal asymmetry in pp elastic scattering," *Phys. Rev.* **C65** (2002) 035502, `arXiv:nucl-th/0109084 [nucl-th]`.

[42] P. Eversheim, W. Schmitt, S. Kuhn, F. Hinterberger, P. von Rossen, *et al.*, "Parity violation in proton proton scattering at 13.6-MeV," *Phys. Lett.* **B256** (1991) 11–14.

[43] D. Nagle, J. Bowman, C. Hoffman, J. McKibben, R. Mischke, *et al.*, "Parity violation in the scattering of 15-MeV protons by hydrogen," *AIP Conf.Proc.* **51** (1979) 224–230.

[44] R. Balzer, R. Henneck, C. Jacquemart, J. Lang, M. Simonius, *et al.*, "Measurement of parity nonconservation in pp scattering at 45-MeV," *Phys. Rev. Lett.* **44** (1980) 699–702.

[45] R. Balzer, R. Henneck, C. Jacquemart, J. Lang, F. Nessi-Tedaldi, *et al.*, "Parity violation in proton-proton scattering at 45-MeV," *Phys. Rev.* **C30** (1984) 1409–1430.

[46] S. Kistryn, J. Lang, J. Liechti, T. Maier, R. Muller, *et al.*, "Precision measurement of parity violation in proton proton scattering at 45-MeV," *Phys. Rev. Lett.* **58** (1987) 1616.

[47] A. R. Berdoz *et al.*, "Parity violation in proton proton scattering at 221-MeV," *Phys. Rev.* **C68** (2003) 034004, `arXiv:nucl-ex/0211020 [nucl-ex]`.

[48] A. R. Berdoz *et al.*, "Parity violation in proton proton scattering at 221 MeV," *Phys. Rev. Lett.* **87** (2001) 272301, `arXiv:nucl-ex/0107014 [nucl-ex]`.

[49] J. Lang, T. Maier, R. Muller, F. Nessi-Tedaldi, T. Roser, *et al.*, "Parity nonconservationin elastic p-alpha scattering and the determination of the weak meson-nucleon coupling constants," *Phys. Rev. Lett.* **54** (1985) 170–173.

[50] R. Henneck, C. Jacquemart, J. Lang, R. Muller, T. Roser, *et al.*, "Study of parity nonconservation in p-alpha scattering," *Phys. Rev. Lett.* **48** (1982) 725–728.

[51] K. Elsener, W. Grubler, V. Konig, P. A. Schmelzbach, J. Ulbricht, B. Vuaridel, D. Singy, C. Forstner, and W. Z. Zhang, "Parity nonconservation in ^{19}F nuclei," *Nucl. Phys.* **A461** (1987) 579–602.

[52] K. Elsener, W. Grubler, V. Konig, P. A. Schmelzbach, J. Ulbricht, D. Singy, C. Forstner, W. Z. Zhang, and B. Vuaridel, "Constraints on weak meson-nucleon coupling from parity nonconservation in F-19," *Phys. Rev. Lett.* **52** (1984) 1476–1479.

[53] C. Wood, S. Bennett, D. Cho, B. Masterson, J. Roberts, *et al.*, "Measurement of parity nonconservation and an anapole moment in cesium," *Science* **275** (1997) 1759–1763.

[54] K. A. Snover, R. von Lintig, E. G. Adelberger, H. E. Swanson, T. A. Trainor, A. B. McDonald, E. D. Earle, and C. A. Barnes, "Upper limit on parity mixing in Ne-21," *Phys. Rev. Lett.* **41** (1978) 145–148.

[55] E. D. Earle, A. B. Mcdonald, E. G. Adelberger, K. A. Snover, H. E. Swanson, R. Von Lintig, H. B. Mak, and C. A. Barnes, "Parity mixing in Ne-21: Evidence for weak neutral currents in nuclei," *Nucl. Phys.* **A396** (1983) 221C–230C.

[56] W. Snow, C. Bass, T. Bass, B. Crawford, K. Gan, *et al.*, "Upper bound on parity-violating neutron spin rotation in He-4," *Phys. Rev.* **C83** (2011) 022501.

[57] V. A. Knyaz'kov, E. A. Kolomenskii, V. A. Lobashov, V. A. Nazarenko, A. N. Pirozhkov, *et al.*, "A new experimental study of the circular polarization of np capture gamma rays," *Nucl. Phys.* **A417** (1984) 209–230.

[58] M. Avenier, J. F. Cavaignac, D. H. Koang, B. Vignon, R. Hart, and R. Wilson, "Parity violation in n-d capture," *Phys. Lett.* **B137** (1984) 125–128.

[59] B. Desplanques, "Parity nonconserving nuclear forces," *Nucl. Phys.* **A335** (1980) 147–167.

[60] C. P. Liu, "Parity-Violating Observables of Two-Nucleon Systems in Effective Field Theory," *Phys. Rev.* **C75** (2007) 065501, `arXiv:nucl-th/0609078 [nucl-th]`.

[61] J. de Vries, N. Li, U.-G. Meißner, A. Nogga, E. Epelbaum, and N. Kaiser, "Parity violation in neutron capture on the proton: Determining the weak pion-nucleon coupling," *Phys. Lett.* **B747** (2015) 299–304, `arXiv:1501.01832 [nucl-th]`.

[62] B. McKellar, "The one pion exchange contribution to the weak parity violating nucleon-nucleon potential," *Phys. Lett. B* **26** (1967) 107–108.

[63] E. Fischbach, "Application of current algebra and partially conserved axial-vector current to the weak B B π vertex," *Phys. Rev.* **170** (1968) 1398.

[64] D. Tadić, "Weak parity-nonconserving potentials," *Phys. Rev.* **174** (1968) 1694.

[65] W. Kummer and M. Schweda, "An SU(6) estimate of the effective nonleptonic parity-violating coupling in strangeness-conserving weak processes," *Acta Phys. Austriaca* **28** (1968) 303–308.

[66] E. Fischbach and D. Tadic, "Parity violating nuclear interactions and models of the weak Hamiltonian," *Phys. Rept.* **6** (1973) 123–186.

[67] M. A. Box, B. H. J. McKellar, P. Pick, and K. R. Lassey, "Parity mixing in nuclei as a test of theories of the weak interaction," *J. Phys.* **G1** (1975) 493.

[68] C. Patrignani, P. D. Group, *et al.*, "Review of particle physics," *Chinese Phys. C* **40** (2016) 100001.

[69] J. F. Donoghue, E. Golowich, and B. Holstein, "Low-energy weak interactions of quarks," *Phys. Repts,* **131** (1986) 319–428.

[70] G. Barton, "Notes on the static parity non-conserving internucleon potential," *Il Nuovo Cimento* **19** (1961) 512–527.

[71] S. L. Glashow, J. Iliopoulos, and L. Maiani, "Weak interactions with lepton-hadron symmetry," *Phys. Rev. D* **2** (1970) 1285.

[72] D. B. Kaplan and M. J. Savage, "An analysis of parity-violating pion-nucleon couplings," *Nucl. Phys. A* **556** (1993) 653–671.

[73] N. Kaiser and U.-G. Meißner, "The weak pion-nucleon vertex revisited," *Nucl. Phys.* **A489** (1988) 671–682.

[74] U. G. Meißner and H. Weigel, "The Parity violating pion nucleon coupling constant from a realistic three flavor Skyrme model," *Phys. Lett.* **B447** (1999) 1–7, `arXiv:nucl-th/9807038 [nucl-th]`.

[75] **MILC** Collaboration, W. Freeman and D. Toussaint, "Intrinsic strangeness and charm of the nucleon using improved staggered fermions," *Phys. Rev.* **D88** (2013) 054503, `arXiv:1204.3866 [hep-lat]`.

[76] **JLQCD** Collaboration, H. Ohki, K. Takeda, S. Aoki, S. Hashimoto, T. Kaneko, H. Matsufuru, J. Noaki, and T. Onogi, "Nucleon strange quark content from $N_f = 2 + 1$ lattice QCD with exact chiral symmetry," *Phys. Rev.* **D87** (2013) 034509, `arXiv:1208.4185 [hep-lat]`.

[77] P. Junnarkar and A. Walker-Loud, "Scalar strange content of the nucleon from lattice QCD," *Phys. Rev.* **D87** (2013) 114510, `arXiv:1301.1114 [hep-lat]`.

[78] **XQCD** Collaboration, M. Gong *et al.*, "Strangeness and charmness content of the nucleon from overlap fermions on 2+1-flavor domain-wall fermion configurations," *Phys. Rev.* **D88** (2013) 014503, `arXiv:1304.1194 [hep-ph]`.

[79] J. Dai, M. J. Savage, J. Liu, and R. P. Springer, "Low-energy effective Hamiltonian for Δ I = 1 nuclear parity violation and nucleonic strangeness," *Phys. Lett.* **B271** (1991) 403–409.

[80] G. Buchalla, A. J. Buras, and M. E. Lautenbacher, "Weak decays beyond leading logarithms," *Rev. Mod. Phys.* **68** (1996) 1125–1144, `arXiv:hep-ph/9512380 [hep-ph]`.

[81] P. A. Boyle, N. H. Christ, N. Garron, E. J. Goode, T. Janowski, *et al.*, "Emerging understanding of the Δ I= 1/2 rule from lattice QCD," *Phys. Rev. Letts.* **110** no. 15, (2013) 152001.

[82] A. J. Buras, J.-M. Gerard, and W. A. Bardeen, "Large N approach to kaon decays and mixing 28 years later: $\Delta I = 1/2$ rule, $\hat{B}_K$ and ΔM_K," *Eur. Phys. J.* **C74** (2014) 2871, `arXiv:1401.1385 [hep-ph]`.

[83] L. Maiani and M. Testa, "Final state interactions from Euclidean correlation functions," *Phys. Lett.* **B245** (1990) 585–590.

[84] K. Huang and C. N. Yang, "Quantum-mechanical many-body problem with hard-sphere interaction," *Phys. Rev.* **105** (1957) 767–775.

[85] T. D. Lee, K. Huang, and C. N. Yang, "Eigenvalues and eigenfunctions of a Bose system of hard spheres and Its low-temperature properties," *Phys. Rev.* **106** (1957) 1135–1145.

[86] T. T. Wu, "Ground state of a Bose system of hard spheres," *Phys. Rev.* **115** (1959) 1390–1404.

[87] M. Luscher, "Volume dependence of the energy spectrum in massive quantum field theories. 2. Scattering states," *Commun. Math. Phys.* **105** (1986) 153–188.

[88] M. Luscher, "Two particle states on a torus and their relation to the scattering matrix," *Nucl. Phys.* **B354** (1991) 531–578.

[89] E. Berkowitz, T. Kurth, A. Nicholson, B. Joo, E. Rinaldi, M. Strother, P. M. Vranas, and A. Walker-Loud, "Two-nucleon higher partial-wave scattering from lattice QCD," *Phys. Lett.* **B765** (2017) 285–292, arXiv:1508.00886 [hep-lat].

[90] B. Tiburzi, "Isotensor hadronic parity violation," *Phys. Rev.* **D86** (2012) 097501, arXiv:1207.4996 [hep-ph].

[91] D. B. Kaplan, M. J. Savage, and M. B. Wise, "A new expansion for nucleon-nucleon interactions," *Phys. Lett.* **B424** (1998) 390–396, arXiv:nucl-th/9801034 [nucl-th].

[92] E. Epelbaum, W. Gloeckle, and U.-G. Meißner, "Nuclear forces from chiral Lagrangians using the method of unitary transformation. 1. Formalism," *Nucl. Phys.* **A637** (1998) 107–134, arXiv:nucl-th/9801064 [nucl-th].

[93] E. Epelbaum, W. Gloeckle, and U.-G. Meißner, "Nuclear forces from chiral Lagrangians using the method of unitary transformation. 2. The two nucleon system," *Nucl. Phys.* **A671** (2000) 295–331, arXiv:nucl-th/9910064 [nucl-th].

[94] U. van Kolck, "Effective field theory of nuclear forces," *Prog. Part. Nucl. Phys.* **43** (1999) 337–418, arXiv:nucl-th/9902015 [nucl-th].

[95] S. R. Beane, P. F. Bedaque, M. J. Savage, and U. van Kolck, "Towards a perturbative theory of nuclear forces," *Nucl. Phys.* **A700** (2002) 377–402, arXiv:nucl-th/0104030 [nucl-th].

[96] E. Epelbaum, H.-W. Hammer, and U.-G. Meißner, "Modern theory of nuclear forces," *Rev. Mod. Phys.* **81** (2009) 1773–1825, arXiv:0811.1338 [nucl-th].

[97] S. R. Beane and M. J. Savage, "Hadronic parity violation on the lattice," *Nucl. Phys.* **B636** (2002) 291–304, arXiv:hep-lat/0203028 [hep-lat].

[98] L. E. Marcucci, K. M. Nollett, R. Schiavilla, and R. B. Wiringa, "Modern theories of low-energy astrophysical reactions," *Nucl. Phys.* **A777** (2006) 111–136.

[99] M. Viviani, R. Schiavilla, L. Girlanda, A. Kievsky, and L. E. Marcucci, "The parity-violating asymmetry in the $^3He(n,p)^3H$ reaction," *Phys. Rev.* **C82** (2010) 044001, arXiv:1007.2052 [nucl-th].

[100] B. Desplanques and J. J. Benayoun, "Parity nonconserving effects in thermal neutron deuteron radiative capture," *Nucl. Phys.* **A458** (1986) 689–708.

[101] V. M. Lobashov, D. M. Kaminker, G. I. Kharkevich, V. A. Kniazkov, N. A. Lozovoy, V. A. Nazarenko, L. F. Sayenko, L. M. Smotritsky, and A. I. Yegorov, "Parity non-conservation in radiative thermal neutron capture by protons," *Nucl. Phys.* **A197** (1972) 241–258.

[102] W. M. Snow *et al.*, "Status of theory and experiment in hadronic parity violation," *Int. J. Mod. Phys. Conf. Ser.* **40** (2016) 1660002.

[103] Y. Avishai and P. Grange, "Parity violation in threshold neutron proton scattering," *J. Phys.* **G10** (1984) L263–L270.

[104] B. Heckel, "PNC and TNC rotations of the neutron spin," in *Proceedings of the Workshop on the Investigation of Fundamental Interactions with Cold Neutrons*, G. L. Greene, ed., p. 90. National Bureau of Standards, 1986.

[105] E. Adelberger, "Parity violation in nuclear systems, scattering and decay experiments," in *Symposium/Workshop on Parity Violation in Hadronic Systems Vancouver, British Columbia, Canada, May 28-29, 1987*, pp. 50–66. 1987.

[106] R. Schiavilla, J. Carlson, and M. W. Paris, "Parity violating interaction effects in the np system," *Phys. Rev.* **C70** (2004) 044007, `arXiv:nucl-th/0404082 [nucl-th]`.

[107] H. W. Griesshammer, M. R. Schindler, and R. P. Springer, "Parity-violating neutron spin rotation in hydrogen and deuterium," *Eur. Phys. J.* **A48** (2012) 7, `arXiv:1109.5667 [nucl-th]`.

[108] R. Schiavilla, M. Viviani, L. Girlanda, A. Kievsky, and L. E. Marcucci, "Neutron spin rotation in n-polarized - d scattering," *Phys. Rev.* **C78** (2008) 014002, `arXiv:0805.3599 [nucl-th]`. [Erratum: Phys. Rev.C83,029902(2011)].

[109] V. F. Dmitriev, V. V. Flambaum, O. P. Sushkov, and V. B. Telitsin, "The parity violating rotation of the neutron spin in helium," *Phys. Lett.* **B125** (1983) 1–4.

[110] B. Desplanques, J. J. Benayoun, and C. Gignoux, "Predictions of parity nonconserving effects in nucleon deuteron scattering," *Nucl. Phys.* **A324** (1979) 221–233.